eLife

Cell Biology

Competition between myosin II and β_H-Spectrin regulates cytoskeletal tension

Consuelo Ibar, Krishna Chinthalapudi, Sarah M. Heissler, Kenneth D. Irvine

Waksman Institute and Department of Molecular Biology and Biochemistry, Rutgers University, Piscataway NJ 08854 USA • Department of Physiology and Cell Biology, Dorothy M. Davis Heart and Lung Research Institute, The Ohio State University College of Medicine, Columbus, Ohio, USA

Reviewed Preprint

Revised by authors after peer review.

About eLife's process

Reviewed preprint version 2
June 26, 2023 (this version)

Reviewed preprint version 1
February 3, 2023

Sent for peer review
December 1, 2022

Posted to bioRxiv
December 1, 2022

Abstract

Spectrins are membrane cytoskeletal proteins generally thought to function as heterotetramers comprising two α-spectrins and two β-spectrins. They influence cell shape and Hippo signaling, but the mechanism by which they influence Hippo signaling has remained unclear. We have investigated the role and regulation of the *Drosophila* β-heavy Spectrin (β_H-Spectrin, encoded by the *karst* gene) in wing imaginal discs. Our results establish that β_H-Spectrin regulates Hippo signaling through the Jub biomechanical pathway due to its influence on cytoskeletal tension. While we find that α-Spectrin also regulates Hippo signaling through Jub, unexpectedly, we find that β_H-Spectrin localizes and functions independently of α-Spectrin. Instead, β_H-Spectrin co-localizes with and reciprocally regulates and is regulated by myosin. In vivo and in vitro experiments support a model in which β_H-Spectrin and myosin directly compete for binding to apical F-actin. This competition can explain the influence of β_H-Spectrin on cytoskeletal tension and myosin accumulation. It also provides new insight into how β_H-Spectrin participates in ratcheting mechanisms associated with cell shape change.

eLife assessment

The manuscript provides **valuable** insights into the regulatory role and mechanisms of the spectrin cytoskeleton in mechanotransduction in *Drosophila*. The data are **compelling** in establishing that alpha and beta spectrin regulate the Hippo signaling pathway independently via their effect on cytoskeletal tension. The work will be of interest to cell and developmental biologists, particularly those who focus on mechanotransduction and the cytoskeleton.

Introduction

The spectrin cytoskeleton has been described as a lattice of cross-linked, spring-like proteins that provide structural support to cells (Liem, 2016; Machnicka et al., 2014). Spectrins were first discovered and characterized in red blood cells but are expressed in many cell types.

Spectrins can bind to cell membranes and F-actin, linking them together. They are generally thought to act as heterotetramers, composed of two α subunits and two β subunits. *Drosophila* has one α-spectrin (α-Spec) and two β-spectrins: β-Spectrin (β-Spec) and β-Heavy-Spectrin (β_H-Spec, encoded by *karst* (*kst*)), which could potentially generate two distinct spectrin heterotetramers: $(\alpha\beta)_2$ and $(\alpha\beta_H)_2$. β-Spec and β_H-Spec interact with F-actin through their N-terminal domains, which contain two actin-binding calponin-homology (CH) domains, connecting the spectrin cytoskeleton to the actin cytoskeleton (Liem, 2016). In *Drosophila* epithelia, it has been reported that β-Spec localizes to the lateral sides of cells, β_H-Spec localizes to the apical sides of cells, and α-Spec localizes both laterally and apically, leading to inferences that spectrin exists as lateral $(\alpha\beta)_2$ tetramers and apical $(\alpha\beta_H)_2$ tetramers (Dubreuil et al., 1997; Lee et al., 1997; Thomas et al., 1998; Zarnescu and Thomas, 1999). Despite common assumptions that spectrins act as tetramers, there is some evidence that alternative arrangements may exist. In *Drosophila* ovarian follicle cells, the absence of α-Spec diminishes the recruitment of β_H-Spec to the apical domain, but it does not affect the recruitment of β-Spec to the lateral domain (Lee et al., 1997). Examination in *Drosophila* of a mutant form of α-Spec that, based on in vitro studies, is unable to bind β-spec and compromised in its ability to bind β_H-Spec, revealed that it could nonetheless rescue the lethality of an *α-Spec* mutant (Khanna et al., 2015). Experiments done with a mammalian homolog of β_H-Spec, βV-Spec, showed that it can homodimerize through its C-terminal region, raising the possibility that βV-Spec might be able to cross-link F-actin by itself (Papal et al., 2013).

Several studies have reported that spectrins also regulate Hippo signaling, with effects on readouts of Hippo signaling reported in *Drosophila* imaginal discs and ovarian follicles, as well as in cultured mammalian cells (Deng et al., 2015; Deng et al., 2020; Fletcher et al., 2015; Wong et al., 2015). Hippo signaling is a signal transduction network that responds to diverse upstream inputs, including the cytoskeleton and cells' physical environment (Misra and Irvine, 2018; Zheng and Pan, 2019). Hippo signaling modulates cell proliferation and fate, largely through the regulation of Yap family transcriptional co-activator proteins (Yorkie, Yki, in *Drosophila*, YAP1 and TAZ in humans). Yki is primarily regulated through phosphorylation by the kinase Warts (Wts), which promotes the cytoplasmic localization of Yki. Various potential mechanisms for biomechanical regulation of Yki/Yap activity have been described, but the best-characterized mechanism in *Drosophila* is the Jub biomechanical pathway. This involves tension-dependent recruitment of an Ajuba LIM protein (Jub in *Drosophila*, LIMD1 in mammals) to α-catenin at adherens junctions (AJ) (Alegot et al., 2019; Ibar et al., 2018; Rauskolb et al., 2022; Rauskolb et al., 2014; Sarpal et al., 2019; Sun et al., 2015). Jub then recruits and inhibits Wts, resulting in increased Yki activity.

Studies of the influence of spectrins on Hippo signaling have suggested different mechanisms by which this might occur (Deng et al., 2015; Deng et al., 2020; Fletcher et al., 2015; Wong et al., 2015). Fletcher et al. (2015), focusing on β_H-Spec, suggested that the spectrin cytoskeleton influences the membrane density, and thereby the activation state, of upstream regulators of Hippo signaling. Wong et al. (2015), focusing on β-Spec, suggested that spectrins might influence Hippo signaling by modulating levels of F-actin; increased levels of F-actin have been reported in other studies to be associated with increased Yki/Yap activity (Aragona et al., 2013; Fernandez et al., 2011; Sansores-Garcia et al., 2011). Deng et al. (2015), focusing on α-Spec, reported that spectrins regulate levels of phosphorylated myosin light chain (required for myosin activation) but surprisingly did not affect levels of myosin or recruitment of Jub, leading them to infer that spectrins can act through a novel tension-dependent but Jub-independent pathway. These same authors later reported that in the pupal eye, spectrins can act through Jub, while suggesting that the action of spectrins in the pupal eye differs from their action in the wing disc (Deng et al., 2015; Deng et al., 2020).

The disparate models for how spectrins influence Hippo signaling have led to confusion over whether a distinct spectrin-based mechanism exists for the mechanical regulation of Hippo signaling. We were particularly interested in investigating claims that spectrins could alter cytoskeletal tension in wing discs without affecting Jub localization or levels of myosin. Our results reveal that both β_H-Spec and α-Spec influence Jub recruitment to AJ, and their effects on Yki activity depend upon Jub. Together, these observations argue that spectrins influence Hippo signaling through the Jub biomechanical pathway. Unexpectedly, our investigations also reveal that β_H-Spec and α-Spec act separately in wing discs – they do not co-localize, nor do they influence each other's localization. These observations argue that β_H-Spec does not act as part of an $(\alpha\beta_H)_2$ tetramer in the wing disc but rather exerts its functions independently of α-Spec. Finally, we establish that β_H-Spec and myosin reciprocally antagonize each other's apical localization in wing discs – myosin inhibits β_H-Spec, and β_H-Spec inhibits myosin. We further show that myosin can compete with β_H-Spec for binding to F-actin in vitro. Together with structural modeling, our observations argue that β_H-Spec and myosin compete with each other for binding to F-actin in vivo. This competition could explain how β_H-Spec influences myosin activity and further suggests a simple mechanism for the contribution of β_H-Spec to ratcheting processes that alter cell shape via actomyosin contractility.

Results

β_H-Spectrin regulates myosin activity and levels in wing imaginal discs

Prior studies have reported that mutation or RNAi-mediated knockdown of spectrins in wing and eye imaginal discs increased myosin activity, as visualized by staining for myosin light chain phosphorylated at activation sites (pMLC) (Deng et al., 2015; Forest et al., 2018). Surprisingly, it was also reported that levels of GFP-tagged myosin light chain (encoded in *Drosophila* by spaghetti squash, Sqh:GFP) or F-actin were nonetheless unaffected (Deng et al., 2015), whereas changes in myosin activity generally correlate with changes in myosin accumulation (Fernandez-Gonzalez et al., 2009; Noll et al., 2017). To re-examine this, we analyzed wing imaginal discs in which the apical, β_H-Spec *kst* was knocked down in posterior wing cells by expressing UAS-RNAi lines under *en-Gal4* control (RNAi validation is presented in Figure 1 – figure supplement 1). This approach leaves unaffected anterior wing disc cells as an internal control. These experiments typically also include a neutral transgene expressed under en-Gal4 control to mark posterior cells (e.g. UAS-RFP) and a transgene expressing Dicer2 (Dcr2) to increase the efficacy of RNAi (Dietzl et al., 2007). This increased apical pMLC in posterior cells, where levels of β_H-Spec were reduced (Figure 1-figure supplement 2B and D), consistent with previous reports (Deng et al., 2015; Forest et al., 2018). A difference in junctional tension between anterior (control) cells and posterior (β_H-Spec RNAi) cells in our experiments was confirmed by measuring the recoil velocity of cell junctions after laser cutting, which demonstrated an increased tension in the β_H-Spec depleted sides (Figure 1G). To examine myosin protein levels, we employed the myosin light chain GFP fusion Sqh:GFP. We found that depletion of β_H-Spec led to increased levels of junctional myosin (Figure 1B). To quantify these effects on Sqh:GFP levels, we made maps of Sqh:GFP intensity normalized against E-cad intensity. These are displayed on a red (high) to blue (low) heat map (Pan et al., 2018) and we also used this analysis to calculate the ratio of intensities of the anterior (control) versus posterior (experimental) compartments (Alegot et al., 2019) (Figure 1D-E, H-I). This was further confirmed by using a distinct β_H-Spec RNAi line

(*UAS-kstRNAi*^{HMS00882}), which similarly increased myosin levels (Figure 1–figure supplement 2E).

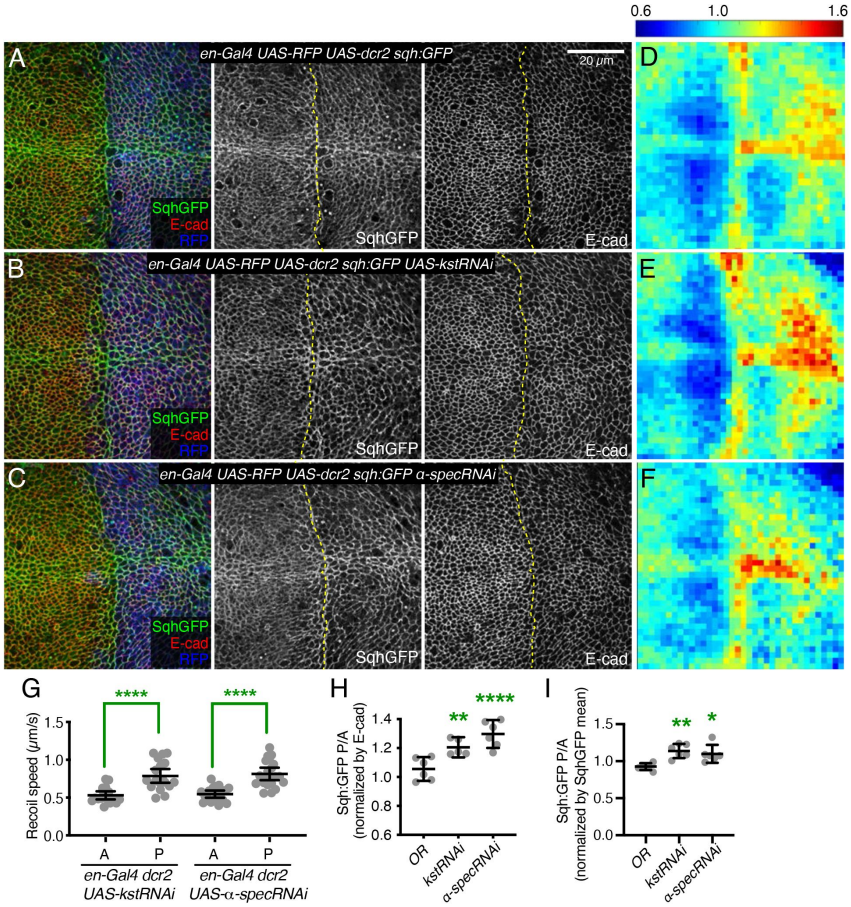

Figure 1.

Knockdown of β_H-Spec or α-Spec increases junctional myosin levels in wing discs

(A-C) Apical sections of wing discs stained for E-cad (red/gray) expressing en-Gal4 UAS-RFP UAS-dcr2 sqh:GFP crossed to control (Oregon-R, OR) (A), UAS-kstRNAi(v37075) (B), or UAS-α-specRNAi (C) showing the effect on Sqh:GFP (green/gray) levels and localization in the posterior compartment (marked by RFP, blue). Dashed yellow line marks A/P compartment boundary. Scale bar = 20 µm; all images are at the same magnification. Panels to the right, in gray, show single channels, as indicated. (D-F) Heat maps of relative junctional Sqh:GFP intensity of wing discs. Average levels of Sqh:GFP relative to E-cad levels are shown for the different genotypes analyzed in A-C. Heat map scale is indicated on the top. Number of wing discs used for analysis: Control (OR), n=6; UAS-kstRNAi, n=5; UAS-α-specRNAi, n=6. (G) Average recoil velocities after laser cutting of cell junctions in anterior (A) or posterior (P) compartments of wing discs expressing UAS-kstRNAi or UAS-α-specRNAi in posterior cells under en-Gal4 control (n=20). (H-I) Quantification of Sqh:GFP normalized to E-cadherin in posterior cells (P) compared to anterior cells (A) in wing disc expressing the indicated constructs, displayed as individual values, normalized by E-cad (H) or normalized by the mean intensity of Sqh:GFP (I). Data are shown as mean ± 95% CI. Statistical significance in (G) was determined by Student's t-test between A and P. For (H) and (I), statistical significance was determined by a one-way ANOVA with Dunnett's multiple comparison test relative to the control (Oregon-R): ns: not significant, *P<0.05; **P≤0.01; ***P≤0.001; ****P≤0.0001.

As earlier studies reporting no effect on myosin levels focused on mutation or knockdown of α-Spec (Deng et al., 2015), we considered the possibility that knockdown of α- and β_H-Spec might differ in their effects on apical myosin accumulation. However, we found that knockdown of α-Spec also caused an increased accumulation of apical myosin, as well as pMLC and junctional tension, similar to the effects of β_H-Spec knockdown (Figure 1C, F, H, I; Figure 1–figure supplement 2C and D). α-Spec and β_H-Spec knockdown differed though in that the thickness of the wing disc epithelium was reduced by α-Spec knockdown, but not by β_H-Spec knockdown (Figure 1–figure supplement 3), indicating that even though α-Spec and β_H-Spec have similar effects on junctional myosin, their roles in wing disc cells differ. Studies in pupal eyes identified a role for α-Spec in attaching F-actin to membranes that was associated with maintaining proper cortical tension and cell shape (Deng et al., 2020); we think the reduced thickness of the epithelium is a reflection of this role in wing discs. That is,

reduced stiffness of the lateral sides of cells when α-Spec is removed may allow cells to expand laterally, and through conservation of volume, simultaneously shorten along the apical-basal axis.

β_H-Spec regulates Hippo signaling through Jub

It was previously argued that spectrins do not influence Hippo signaling through the Jub biomechanical pathway in wing discs, in part based on an apparent lack of effect of α-*Spec* mutation or depletion on Jub localization (Deng et al., 2015). However, multiple studies have consistently observed that Jub localization increases when tension at AJ is increased (Forest et al., 2018; Pan et al., 2018; Rauskolb et al., 2019; Rauskolb et al., 2014; Razzell et al., 2018). Thus, we examined Jub localization under conditions of β_H-Spec depletion. In wing imaginal discs, Jub accumulates in puncta that often occur near intercellular vertices, together with a lower-level, more even accumulation along the cell-cell junctions (Figure 2A and Figure 2–figure supplement 1B). Jub is recruited by a tension-dependent conformational change of α-catenin, and Jub puncta are increased when cytoskeletal tension is higher. Consistent with this, examination of Jub:GFP confirmed that the increased junctional tension and myosin activity caused by β_H-Spec depletion is associated with increased junctional recruitment of Jub (Figure 2B, E, G-H and Figure 2-figure supplement 1C).

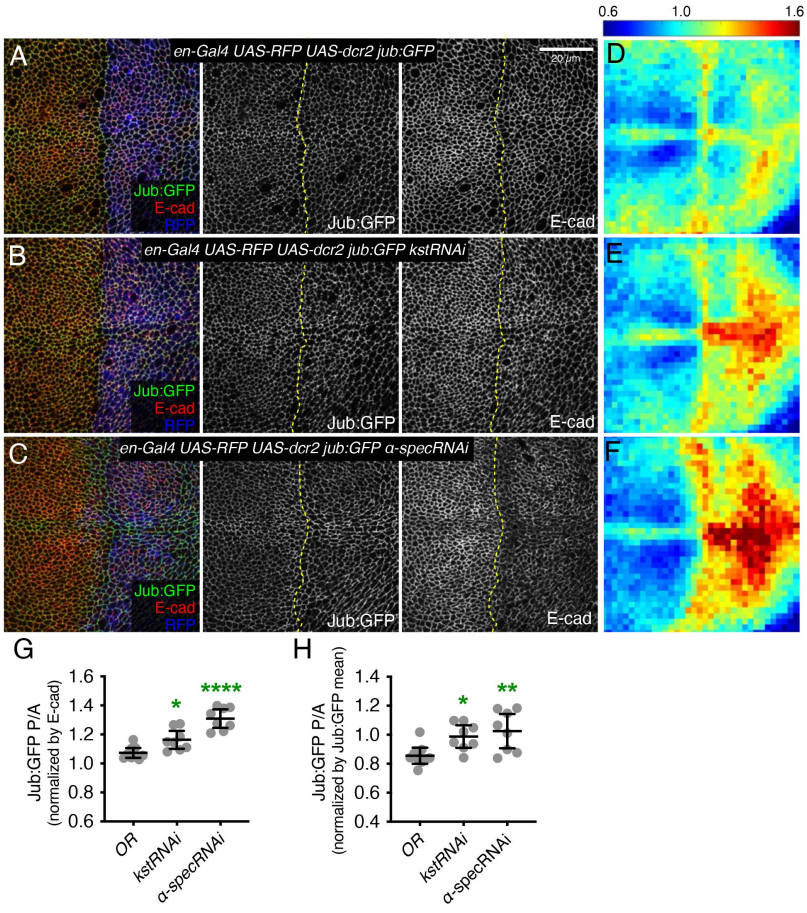

Figure 2.

Knockdown of β_H-Spec or α-Spec increases junctional Jub levels in wing discs (A-C) Apical sections of wing discs expressing en-Gal4 UAS-RFP UAS-dcr2 Jub:GFP crossed to control (Oregon-R, OR) (A), UAS-kstRNAi(v37075) (B) or UAS-α-specRNAi (C) stained for E-cad (red/gray) showing the effect on Jub:GFP (green/gray) in the posterior compartment (marked by RFP, blue). Dashed yellow line marks the A/P compartment boundary. Panels to the right, in gray, show single channels, as indicated. Scale bar = 20 µm. (D-F) Heat maps of relative junctional Jub:GFP intensity of wing discs. Levels of Jub:GFP relative to E-cad levels are shown for the different genotypes analyzed. Heat map scale is indicated on the top. Number of wing discs used for analysis: Control (OR), n=9; UAS-kstRNAi, n=8; UAS-α-specRNAi, n=8. (G-H) Quantification of Jub:GFP normalized to E-cadherin (G) or to Jub:GFP mean intensity (H) in posterior cells compared to anterior cells (P/A) in wing discs expressing the indicated constructs, displayed as individual values. Data are shown as mean ± 95% CI. Statistical significance was determined by one-way ANOVA with Dunnett's multiple comparison test relative to the control (Oregon-R): ns: not significant, *P<0.05; **P≤0.01; ***P≤0.001; ****P≤0.0001

To assess the functional significance of increased Jub localization to AJ under β_H-Spec knockdown conditions, we assayed the ability of RNAi-mediated *jub* knockdown to suppress β_H-Spec (kst) RNAi phenotypes. Knockdown of β_H-Spec throughout the developing wing under *nub-Gal4* control increases wing size (wings were 116% and 119% of *nub-Gal4 UAS-dcr2* control size for the two different UAS-RNAi lines used) (Figure 3A, C-D and K) (Deng et al., 2015; Fletcher et al., 2015). Knockdown of *jub* leads to smaller wings (Das Thakur et al., 2010; Rauskolb et al., 2011). In animals with simultaneous RNAi knockdown of *jub* and *kst,* wing size is similar to that of *jub* RNAi wings (Figure 3B, E-F and K). The epistasis of *jub* to *kst* is consistent with the hypothesis that β_H-Spec regulates wing size through its tension-dependent regulation of Jub. To further illustrate this, we reduced tension in wing discs with β_H-Spec knockdown by simultaneous RNAi knockdown of *Rho kinase (Rok)* (Rauskolb et al., 2014; Winter et al., 2001). This reduced wing size and junctional Jub localization similar to that observed in control wing discs with *Rok* knockdown (Figure 3-figure supplement 1) (Rauskolb et al., 2014).

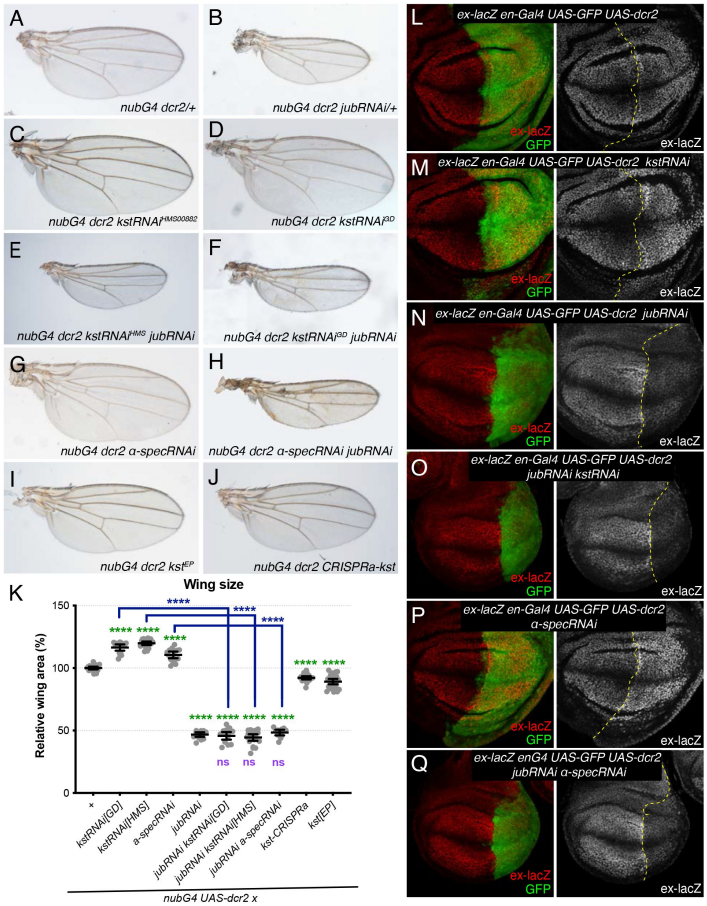

Figure 3.

Jub is required for β_H-Spec and α-Spec regulation of wing size and ex-lacZ

(A-J) Representative adult wings from flies cultured at 29°C and expressing UAS transgenes altering spectrin and/or Jub expression under control of a nub-Gal4 (nubG4) driver. (K) Quantification of wing area (mean ± 95% CI) Number of wing discs used for analysis: Control (OR), n=20; UAS-kstRNAi[GD], n=20; UAS-kstRNAi[HMS], n=21; UAS-α-specRNAi, n=20; UAS-jubRNAi, n=20, UAS-jubRNAi UAS-kstRNAi[GD], n=20; UAS-jubRNAi UAS-kstRNAi[HMS], n=20; UAS-jubRNAi UAS-α-specRNAi, n=20; UAS-kstCRISPRa, n=22; UAS-kst[EP], n=26. Statistical significance was determined by a one-way ANOVA with Tukey's multiple comparison test. Statistical comparisons are shown relative to nub-Gal4 UAS-dcr2/+ in green, relative to nub-Gal4 UAS-dcr2 UAS-jubRNAi in purple and relative to UAS-kstRNAi in blue. (L-Q) Third-instar wing discs expressing ex-lacZ en-Gal4 UAS-dcr2 UAS-GFP (green) crossed to OR (L), UAS-kstRNAi (M), UAS-jubRNAi (N), UAS-jubRNAi UAS-kstRNAi (O), UAS-α-specRNAi (P), UAS-jubRNAi UAS-α-specRNAi (Q) stained for expression of ex-lacZ (red/white). Dashed yellow line indicates the A/P compartment boundary.

To confirm that the relationship between Jub and β_H-Spec revealed by analysis of adult wing size corresponds to changes in Hippo pathway activity, we analyzed the expression of a transcriptional reporter of *expanded (ex)*, *ex-lacZ*, which is a direct target of Yki (Hamaratoglu et al., 2006). Knockdown of β_H-Spec in posterior compartments through the expression of UAS-*kst* RNAi under *en-Gal4* control caused a mild increase in *ex-lacZ* expression compared to the anterior compartment and to control posterior compartments

(Figure 3L,M) (Fletcher et al., 2015). Knockdown of *jub* reduces *ex-lacZ* expression (Das Thakur et al., 2010; Rauskolb et al., 2011). Simultaneous RNAi knockdown of *jub* and *kst* reduced *ex-lacZ* expression, similar to that in *jub* RNAi cells (Figure 3N,O). The suppression of the influence of *kst* on Hippo signaling is again consistent with the inference that β_H-Spec regulates Hippo signaling through the Jub biomechanical pathway.

As claims that spectrins act independently of Jub in wing discs were based primarily on analysis of α-Spec, we also examined the effect of α-Spec knockdown on Jub levels. When α-Spec was knocked down in posterior cells by *en-Gal4* driven RNAi, we observed that recruitment of Jub to cell junctions was increased (Figure 2C, F-H). Moreover, as for β_H-Spec, we found that the increased wing size and *ex-lacZ* expression caused by knockdown of α-Spec were suppressed by knockdown of *jub* (Figure 3G, H, K and P,Q). Thus, as for β_H-Spec, and as suggested for pupal eyes (Deng et al., 2020), our observations imply that α-Spec also regulates Hippo signaling through Jub in wing discs.

β_H-Spec localizes independently from α-Spec in wing disc cells

Prior studies of spectrin function in imaginal discs have assumed that they function as heterotetramers, with an apical complex composed of $(\alpha\beta_H)_2$ subunits and a lateral complex composed of $(\alpha\beta)_2$ subunits (Deng et al., 2015; Deng et al., 2020; Fletcher et al., 2015; Thomas et al., 1998), as was originally suggested for ovarian follicle cells (Lee et al., 1997). However, our examination of spectrin localization in wing imaginal discs suggested that the apical-most distributions of α-Spec and β_H-Spec differ. To directly compare them, we used an antibody against α-Spec (Dubreuil et al., 1987) and a fully functional genomic YFP-trap of β_H-Spec (Kst:YFP) (Lye et al., 2014). β_H-Spec is localized, as reported previously, at the apicobasal level of the adherens junction in wing discs (Fletcher et al., 2015; Forest et al., 2018) (Figure 4A, C). Conversely, α-Spec is enriched in a sub-apical region just below this, with slightly lower levels extending all along the lateral membrane (Figure 4B, C). Only very low levels of α-Spec are detected in the apical plane where β_H-Spec is detected, and their distributions in this plane appear to differ (Figure 4A).

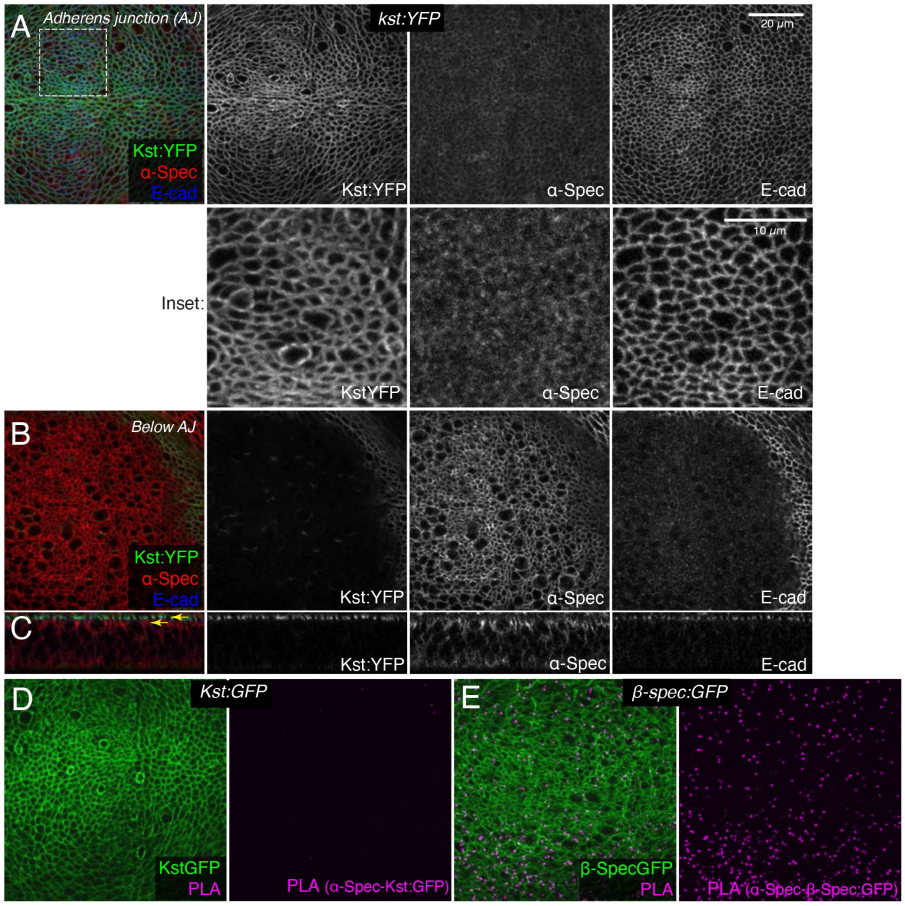

Figure 4.

β_H-Spec and α-Spec do not co-localize in wing discs.

(A-C) Wing discs expressing Kst:YFP immunostained with α-Spec (red/gray) and E-cad (blue/gray) antibodies showing the localization of β_H-Spec (Kst:YFP, green/gray) and α-Spec at the AJ (A), below the AJ (B) and in cross sections (C). Upper yellow arrow in cross section indicates AJ layer, lower yellow arrow indicates "Below AJ" layer. Inset shows higher magnification of single channels from the boxed region in A. (D,E) Wing discs expressing Kst:GFP (D) or β-spec:GFP (E), with GFP in green and signal from Proximity Ligation Assays (PLA) using rabbit anti-GFP and mouse α-Spec antibodies in magenta.

To confirm that β_H-Spec and α-Spec localize independently of each other in wing discs, we examined the consequences of depleting α-Spec, β-Spec, or β_H-Spec on each other's localization. For this, we used *en-Gal4* driven UAS-RNAi lines to knockdown one of the spectrin proteins, and then examined whether the localization of the others was affected. These experiments revealed, as expected, that β-Spec is not required for β_H-Spec localization (Figure 5B), but it does strongly reduce α-Spec localization (Figure 5E). α-Spec is not required for β_H-Spec localization (Figure 5A) but its knockdown slightly reduces β-Spec localization (Figure 5D). Finally, β_H-Spec depletion does not affect α-Spec localization (Figure 5C). These observations suggest that while α-Spec needs β-Spec to localize to lateral membranes, the localization of β_H-Spec and α-Spec are functionally independent. To further examine the relationship between spectrins, we performed proximity ligation assays using antibodies against α-Spec and GFP. A PLA signal consistent with close association of α-Spec and β-Spec was observed in wing discs expressing GFP-tagged β-Spec (Fig. 4E). Conversely, no significant PLA signal was detected in wing discs expressing GFP-tagged β_H-Spec, implying that α-Spec and β_H-Spec are not closely associated in wing discs (Figure 4D). Together with the distinct localization of these proteins revealed by imaging, these observations argue against the existence of $(\alpha\beta_H)_2$ complexes in wing imaginal discs.

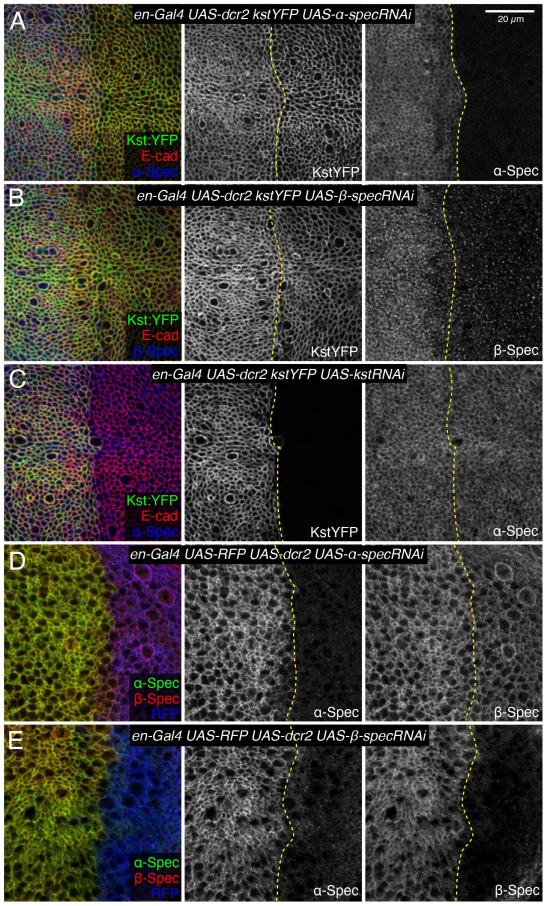

Figure 5.

Influence of spectrin knockdowns on spectrin subunit localization in wing discs.

(A-C) Apical sections of wing discs expressing en-Gal4 UAS-dcr2 Kst:YFP (green/gray) along with UAS-α-specRNAi (A), UAS-β-specRNAi (B) and UAS-kstRNAi (C) immunostained for α-Spec (A and C, blue/gray) or β-Spec antibodies (B, blue/gray). The AJ layers were obtained by ImSAnE, using as a reference the E-cad channel and 7 layers were projected (2.1 μm). (D,E) Sections of wing discs expressing en-Gal4 UAS-RFP (blue) UAS-dcr2 crossed with UAS-α-specRNAi (D) or UAS-β-specRNAi (E) stained with mouse α-Spec (green/gray) and rabbit β-Spec antibody (red/gray) . Dashed yellow lines indicate the A/P compartment boundary. Scale bar = 20 μm.

β_H-Spec and apical myosin antagonize each others' localization to apical F-actin

The discovery that β_H-Spec and α-Spec localize independently led us to consider what factors might influence the apical localization of β_H-Spec. Intriguingly, the distribution of β_H-Spec in wing disc cells appears very similar to the apical distribution of F-actin and myosin, and similarities between the localization of β_H-Spec and myosin in *Drosophila* embryos have been noted previously (Krueger et al., 2020; Thomas and Kiehart, 1994). To determine whether myosin and β_H-Spec colocalize in wing discs, we imaged discs expressing GFP-tagged β_H-Spec (Kst:GFP) and mCherry-tagged myosin light chain (sqh-Sqh:mCherry). This revealed extensive co-localization between these proteins in the apical region of wing disc epithelial cells (Figure 6A, B). Quantitation of these images yielded a Pearson's Correlation Coefficient score of 0.636. For comparison, the Pearson's Correlation Coefficient score between Kst:YFP and α-Spec (Figure 4A) was 0.18. Both Kst:GFP and Sqh:mCherry also colocalized with F-actin, with Pearson's Correlation Coefficient scores of 0.641 and 0.612, respectively.

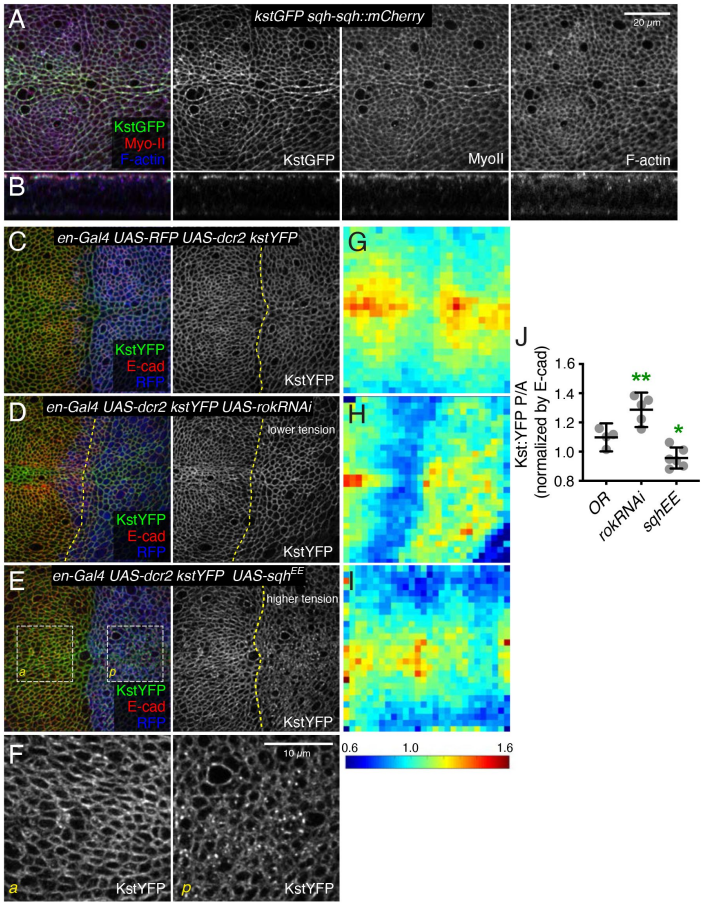

Figure 6.

βH-Spec colocalizes with myosin and is regulated by myosin activity

(A,B) Wing disc co-expressing Kst:GFP (green/gray) and the labelled myosin II subunit sqh:mCherry (red/gray) in apical horizontal sections (A) and lateral sections (B), co-stained with phalloidin for F-actin (blue/gray). (C-E) Apical sections of wing discs expressing en-Gal4 UAS-RFP UAS-dcr2 kst:YFP crossed to (Oregon R, OR) (C), UAS-rokRNAi (D) or UAS-sqhEE (E) in the posterior compartment (marked by RFP, blue), showing the effect of altering myosin activity on Kst:YFP. Dashed yellow lines lines mark the A/P compartment boundary. Scale bar = 20 µm. (F) Higher magnification of the boxed regions indicated in E. Scale bar = 10 µm (G-I) Heat maps of junctional Kst:YFP intensity relative to E-cad in en-Gal4 UAS-RFP UAS-dcr2 kst:YFP crossed to (Oregon R, OR) (C), UAS-rokRNAi (D) or UAS-sqhEE (E) wing discs (n=5 for each genotype), as in the representative examples shown in C to E. Heat map scale is at bottom. (J) Quantification of Kst:YFP intensity normalized to E-cadherin in posterior cells (P) compared to anterior cells (A) in wing discs expressing the indicated constructs under en-Gal4 control (n=5). Data are shown as mean ± 95% CI, error bars indicate CI. Statistical significance was determined by a one-way ANOVA with Dunnett's multiple comparison test relative to the control (Oregon-R): ns: not significant, *P<0.05; **P≤0.01.

The extensive co-localization of β_H-Spec and myosin prompted us to investigate the functional relationship between them further. As noted above, reduction of β_H-Spec leads to increased apical myosin levels and activity. To investigate whether myosin reciprocally regulates β_H-Spec, we expressed transgenes that modulate actomyosin contractility. RNAi-mediated knockdown of Rok reduces myosin activity by reducing phosphorylation of myosin light chain (Winter et al., 2001). In wing discs, knockdown of *Rok* is also associated with reduced recruitment of myosin to apical junctions and reduced junctional tension (Rauskolb et al., 2014) (Figure 6 – figure supplement 1C), consistent with the generally positive correlation between myosin activity and co-localization with F-actin (Fernandez-Gonzalez et al., 2009; Noll et al., 2017). Conversely, examination of β_H-Spec in wing disc cells expressing *Rok* RNAi revealed increased levels of β_H-Spec along apical junctions (Figure 6D). To increase myosin activity, we expressed a constitutively activated, phosphomimetic form of myosin light chain, Sqh^{EE} (Winter et al., 2001). This increases the recruitment of myosin to AJ and increases junctional tension (Rauskolb et al., 2014) (Figure 6 – figure supplement 1D), but decreases the recruitment of β_H-Spec to AJ, and a portion of β_H-Spec instead appears in apical vesicles (Figure 6E,F). To quantify these effects on β_H-Spec levels, we made maps of β_H-Spec intensity normalized against E-cad intensity, displayed on a red (high) to blue (low) heat map. Calculation of the ratio of intensities of the anterior (control) versus posterior (experimental) compartments further confirmed our observation that myosin antagonizes

localization of β_H-Spec to AJ (Figure 6G-J). Thus, β_H-Spec and myosin II localization to AJ are affected in opposite ways by changes in cytoskeletal tension.

The opposing effects of changes in myosin activity on myosin and β_H-Spec localization, together with the observation that loss of β_H-Spec leads to increased myosin activity and apical localization, raised the possibility that myosin and β_H-Spec compete for localization to apical F-actin. To further investigate this possibility, we overexpressed β_H-Spec using a CRISPR-activator (CRISPRa) approach. This involves the expression of a transcriptional activator fused to dCas9 under UAS control, which can then be recruited to a gene of interest using a single-guide RNA (sgRNA) targeted upstream of the transcription start site (Jia et al., 2019; Jia et al., 2018). To verify the overexpression of β_H-Spec, we employed it in flies with GFP-tagged β_H-Spec at the endogenous locus (Kst:GFP). To avoid excessive cell death caused by Kst overexpression we expressed this construct under inducible conditions, using the temperature-sensitive Gal4 repressor Gal80^{ts}. Both imaging and western blotting of wing discs confirmed that this CRISPRa approach effectively increased expression of Kst:GFP (Figure 7 – figure supplemental 1A-B). Examination of myosin under β_H-Spec overexpression conditions, using Sqh:GFP, revealed a substantial reduction of myosin localization to AJs (Figure 7A, C, E-F), and a reduction in tension along cell junctions as assayed by the recoil speed after laser cutting (Figure 7I). Apical cell areas were also increased, consistent with a reduction of junctional tension (Figure 7B and Fig 7-supplement 1). As an independent method to overexpress β_H-Spec, we used a previously described EP-element insertion near *kst*, P[EPgy2]EY01010 (UAS-kst^{EP}) (Pogodalla et al., 2021). Over-expression of β_H-Spec using UAS-kst^{EP} under *en-Gal4* control also reduced myosin levels at AJ (Figure 7 – figure supplement 1C), although the effect appeared weaker than that induced by the CRISPRa approach. These results provide further evidence that β_H-Spec antagonizes myosin recruitment to AJs and establish that this effect can be observed under both increased and decreased β_H-Spec expression conditions. Consistent with these reductions in apical myosin accumulation, β_H-Spec overexpression also reduced junctional recruitment of Jub (Figure 7B,D,G,H and Figure 7 – figure supplement 1D) and decreased wing size (wings were 92% and 89% of *nub-Gal4 UAS-dcr2* control size, for the two different overexpression constructs) (Figure 3I-K).

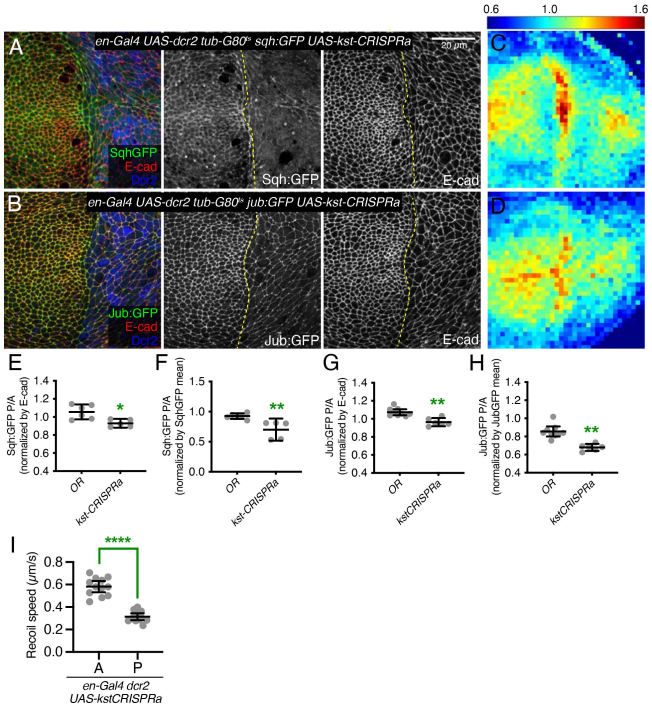

Figure 7.

β_H-Spec overexpression reduces in junctional tension in wing discs.

(A-B) Apical sections of wing imaginal discs expressing en-Gal4 UAS-RFP UAS-dcr2 sqh:GFP (A) or en-Gal4 UAS-RFP UAS-dcr2 jub:GFP (B) crossed to UAS-kst-CRISPRa showing the effect on Sqh:GFP or Jub:GFP levels and localization in the posterior compartment (marked by RFP, blue). Yellow dashed line indicates the A/P compartment boundary. Scale bar = 20 µm; all images are at the same magnification. (C-D) Heat maps of relative junctional Sqh:GFP (C) or Jub:GFP (D) intensity of wing discs. Levels of Sqh:GFP relative to E-cad levels are shown for the different genotypes analyzed in A-B. Heat map scale is indicated on the top. Number of wing discs used for analysis: UAS-kst-CRISPRa with Sqh:GFP, n=5; UAS-kst-CRISPRa with Jub:GFP, n= 6 (E-F) Quantification of Sqh:GFP overlapping E-cad in posterior cells (P) compared to anterior cells (A) in wing disc expressing the indicated

constructs, displayed as individual values, normalized by E-cad (E) or normalized by the mean intensity of Sqh:GFP (F). (G-H) Quantification of Jub:GFP overlapping E-cad in posterior cells (P) compared to anterior cells (A) in wing disc expressing the indicated constructs, displayed as individual values, normalized by E-cad (G) or normalized by the mean intensity of Jub:GFP (H). (I) Average recoil velocities after laser cutting of cell junctions in anterior (A) or posterior (P) compartments of wing discs expressing UAS-kstCRISPRa in posterior cells (n=20). Data are shown as mean ± 95% CI. Statistical significance in (I) was determined by Student's t-test between A and P. For (J) and (K), statistical significance was determined by a one-way ANOVA with Dunnett's multiple comparison test relative to the control (Oregon-R): ns: not significant, *P<0.05; **P≤0.01; ***P≤0.001; ****P≤0.0001.

β_H-Spec and myosin compete for binding to F-actin

The reciprocal antagonism between myosin and β_H-Spec suggested that they could compete for binding to F-actin. β_H-Spec contains two N-terminal actin-binding domains, CH1 and CH2 (Liem, 2016), and myosin contains an actin-binding region in its motor domain (Duan et al., 2018). While spectrins and myosin have been purified and characterized in vitro, we lack a mechanistic understanding of the interaction between β_H-Spec and F-actin and how it might affect myosin binding. To address this, we conducted in vitro co-sedimentation assays with purified protein domains and F-actin. We found that the isolated *Drosophila* β_H-Spec actin-binding region binds F-actin weakly (Figure 8A), in agreement with previous reports of F-actin binding by other spectrin CH1-CH2 domains (Avery et al., 2017; Duan et al., 2018). Constitutively active *Drosophila* Myosin II (subfragment-1-like protein) binding to F-actin appears stronger than β_H-Spec binding, as at the same concentration a greater fraction of Myosin II is bound to F-actin (Figure 8A,B). To investigate the antagonism between these proteins observed in vivo, we performed biochemical competition assays between the β_H-Spec CH domains and myosin for binding to F-actin. F-actin was preincubated with an excess of β_H-Spec CH domains to maximize binding to F-actin, and then increasing concentrations of myosin were added. We found that myosin can displace the actin-binding region of β_H-Spec from F-actin by ~50% at the highest myosin concentration that we could use (Figure 8C, bottom right). Myosin binding to F-actin was unaffected by preincubation with β_H-Spec CH domains (Figure 8 – figure supplement 1A), likely due to active myosin's higher binding affinity for F-actin.

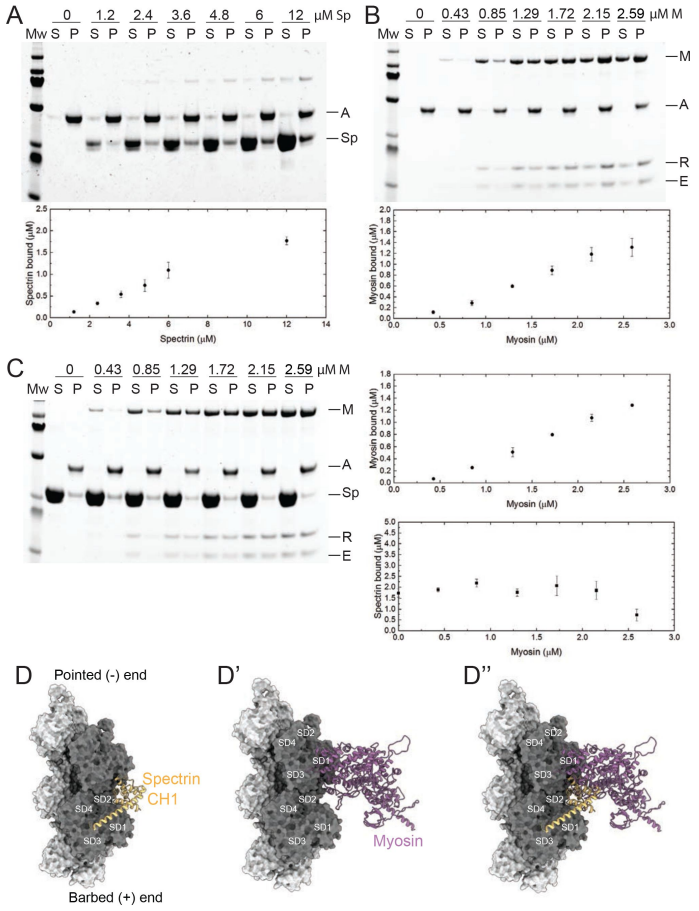

Figure 8.

β_H-Spec and myosin have overlapping binding sites on F-actin.

(A-C) Co-sedimentation assays with βH-Spec CH domains (Spectrin), F-actin, and myosin-II subfragment-1-like protein (myosin). For all sedimentation assays, A, M, Sp, E, and R refer to F-actin, myosin heavy chain, spectrin, myosin essential light chain and myosin regulatory light chain, respectively. Mw indicates marker and S and P refer to supernatant and pellet, respectively. Quantification shows mean ± S.D. of the sedimentation behavior of spectrin and myosin with F-actin (n = 3). (A) Co-sedimentation assay between spectrin (0-12 µM) and F-actin (2 µM). (B) Co-sedimentation assay between myosin (0-2.59 µM) and F-actin (2 µM). (C) Co-sedimentation assay between spectrin (12 µM), myosin (0-2.59 µM) and F-actin (2 µM). Quantification shows that myosin reduces spectrin binding by ~50% (bottom panel). (D-D'') Model of the *Drosophila* CH1 domain (yellow) bound to F-actin (grey) (D). Model of the *Drosophila* myosin motor domain (purple) bound to F-actin (grey) (D'). Superimposition of the CH1 and myosin motor domain on F-actin. The two strands of the actin filament are shown in light and dark grey and subdomains are indicated.

To gain a structural understanding of the antagonism between β_H-Spec and myosin we built homology models of the *Drosophila* CH1-CH2 domain of β_H-Spec and the myosin II motor domain and compared them with previous cryo-EM structures of the human actin-bound β-III-spectrin actin binding CH1 domain and actin-bound myosin (Avery et al., 2017; von der Ecken et al., 2016). The superimposition of the isolated *Drosophila* β_H-Spec CH1 domain model on the human β-III spectrin CH1 domain in a complex with F-actin structure revealed a binding site between actin subdomains (SD) SD1 and SD2 along the filament (Figure 8D). The binding region of myosin on F-actin includes SD1, SD2, and SD3 (Figure 8D'). The superimposition of both models suggests that the binding position of the CH1 domain on F-actin sterically interferes with the formation of a strong actin-myosin interface (Figure 8D''). Modeling of the β_H-Spec CH1-CH2 domain indicates that the CH2 domain presents additional steric hindrance for myosin binding to F-actin (Figure 8 – figure supplement 1B-B''). Thus, structural modeling suggests that the binding of spectrin or myosin to individual binding sites on F-actin is mutually exclusive, which could explain why they compete for F-actin association in vivo and in vitro.

Discussion

Multiple models for how spectrins regulate Hippo signaling have been proposed (Deng et al., 2015; Deng et al., 2020; Fletcher et al., 2015; Wong et al., 2015). We focused on investigating claims that spectrins could alter cytoskeletal tension in wing discs by regulating pMLC levels without affecting localization of myosin or Jub (Deng et al., 2015). In contrast to prior studies, we observed that when β_H-Spec or α-Spec levels are decreased by RNAi, levels of junctional myosin are increased. This increase in junctional myosin levels is associated with increased junctional tension and with increased recruitment of Jub to AJ. We are not certain why these effects were missed in prior studies, but we note that our observations are consistent with studies linking recruitment of both myosin and Jub to AJ under tension (Alegot et al., 2019; Fernandez-Gonzalez et al., 2009; Ibar et al., 2018; Noll et al., 2017; Rauskolb et al., 2019; Rauskolb et al., 2014; Razzell et al., 2018; Sarpal et al., 2019). Moreover, our results are further supported by the observation that *jub* is genetically required for the influence of spectrin knockdown on Yki activity and wing growth. Taken together, these observations imply that β_H-Spec and α-Spec regulate Hippo signaling in wing discs through the Jub-biomechanical pathway, rather than through hypothesized alternate mechanisms.

Spectrin has been suggested to form two distinct complexes in *Drosophila* epithelial cells, $(\alpha\beta)_2$ and $(\alpha\beta_H)_2$ heterotetramers, which localize to the lateral and apical sides of cells, respectively (Deng et al., 2015; Dubreuil et al., 1997; Fletcher et al., 2015; Lee et al., 1997; Thomas et al., 1998; Zarnescu and Thomas, 1999). However, our observations indicate that β_H-Spec functions independently of α-Spec in wing imaginal discs. α-Spec and β_H-Spec do not exhibit significant co-localization. Moreover, α-Spec and β_H-Spec are not required for each other's localization to apical cell junctions. This contrasts with the requirement for β-Spec for recruitment of α-Spec to lateral membranes in wing discs. The requirement is not entirely reciprocal, as α-Spec knockdown only partially reduces β-Spec recruitment, but this likely reflects mechanisms that recruit spectrins to cell membranes: β-spectrin subunits, but not α-spectrin subunits, have a pleckstrin homology domain that can mediate membrane association, as well as possessing the CH domains that mediate F-actin association. Thus β-Spec can associate with lateral membranes without α-Spec, but α-Spec does not have a way to associate with lateral membranes without β-Spec.

An independent role for β_H-Spec has also been suggested in mammalian photoreceptors, where it was reported that that mammalian βV-Spec does not colocalize with αII-Spectrin, and that βV-Spec could form homodimers, potentially allowing it to cross-link actin by itself, enabling α-Spec-independent functions (Papal et al., 2013). The observation that a mutation in *Drosophila* α-Spec that disrupts binding to β-Spec *in vitro* has only mild phenotypes also suggests that spectrin functions do not depend entirely on αβ interactions (Khanna et al., 2015). Collectively, our results together with these earlier studies emphasize that the dogma that "Spectrin comprises α-and β-subunits that interact in an antiparallel manner to form an αβ dimer" (Liem, 2016) should be revised. Nonetheless, our results do not exclude the possibility that β_H-Spec and α-Spec might act together in a physical complex in other tissues, or under distinct physiological conditions.

The conclusion that β_H-Spec and α-Spec act independently in wing discs implies that they influence tension at apical junctions through distinct mechanisms. We suggest that α-Spec could influence AJ tension in wing discs through the mechanism proposed to explain the influence of α-and β-Spec in pupal eyes (Deng et al., 2020). It was inferred that α-and β-Spec maintain cell rigidity by linking F-actin to membranes. In the absence of α-or β-Spec, it was proposed that dissociation between F-actin and the membrane leads to an expansion of the apical regions. This expansion increases cytoskeletal tension at AJs, which bind F-actin independently of spectrins. Consistent with this suggested mechanism, we observed a

decrease in cell height in α-Spec knockdown cells in wing discs, in conjunction with increased tension at apical junctions. The alteration in cell shape was not observed in β_H-Spec knockdown cells, further supporting the conclusion that β_H-Spec and α-Spec act in different ways to regulate junctional tension.

Instead, our experiments analyzing the relationship between β_H-Spec and myosin revealed an entirely different mechanism by which β_H-Spec influences tension at AJ. We observed a mutual antagonism between β_H-Spec and myosin *in vivo* for localization to apical F-actin: decreasing β_H-Spec increases junctional myosin, while increasing β_H-Spec decreases junctional myosin. Reciprocally, increasing myosin activity decreases β_H-Spec localization to apical F-actin, while decreasing myosin activity increases β_H-Spec localization to apical F-actin. In vitro studies with purified protein domains revealed that myosin can compete with β_H-Spec for binding to F-actin. Finally, computational modeling of protein structures revealed that myosin and β_H-Spec would interfere with each other's binding to F-actin. Together, these observations indicate that β_H-Spec and myosin can directly compete with each other for localization to F-actin. We suggest therefore that the influence of β_H-Spec on junctional tension is likely to be a direct consequence of its competition with myosin for overlapping binding sites on F-actin.

Despite β_H-Spec and myosin sharing overlapping binding sites on F-actin, and competing reciprocally in vivo, in our co-sedimentation experiments we could only detect a partial ability of myosin to compete for β_H-Spec binding, and we could not detect an ability of β_H-Spec to compete for myosin binding. Several factors are likely to contribute to these observations. First, we could not use higher protein concentrations of myosin or β_H-Spec due to the need to keep the salt concentration constant and close to physiological levels, and to prevent protein precipitation. Second, it has been suggested for β-Spec that the CH2 domain regulates the actin binding function of the CH1 domain through steric hindrance when the two domains are associated (Avery et al., 2017). A specific mutation in β-Spec CH2 (L253P) has been shown to lower the energetic barrier between closed and open structural states, increasing the affinity of β-Spec for F-actin around 1000-fold (Avery et al., 2016), but it is unknown how β-Spec or β_H-Spec conformational changes are normally regulated in vivo and whether both proteins share this regulatory feature. Additionally, phosphorylation of myosin regulatory light chain shifts myosin from a compact, autoinhibited conformation to a filamentous, active conformation (Kiehart and Feghali, 1986; Vasquez et al., 2016). The autoinhibited conformation binds F-actin very weakly (K_D>100 μM) (Heissler and Manstein, 2013; Sellers et al., 1982) compared to the active conformation, suggesting that spectrin could outcompete autoinhibited myosin more effectively than active myosin for binding to F-actin. Our in vitro experiments used an active form of myosin. In addition, other factors including other actin-binding proteins and cytoskeletal tension are likely to influence the dynamic localization and actin-binding properties of both proteins (Duan et al., 2018; Greenberg et al., 2016).

The competition between β_H-Spec and myosin also provides key insights into how β_H-Spec contributes to ratcheting of apical constriction. The apical constriction of cells in the ventral furrow that initiates *Drosophila* mesoderm invagination occurs through fast constriction pulses interrupted by pauses during which cells must stabilize their constricted state before reinitiating constriction (Martin et al., 2009; Xie and Martin, 2015). This ratcheting-like behavior is thought to be a consequence of the finite length of actin filaments. Myosin contracts the cytoskeleton by driving filaments past each other, and extensive contractions require release and reassociation with new pairs of filaments. β_H-Spec participates in ratcheting of apical constriction (Krueger et al., 2020). When β_H-Spec is knocked down, cells can undergo cycles of unratcheted apical constriction during which they alternately constrict and then expand. Consequently, most β_H-Spec depleted embryos fail to complete normal mesoderm invagination. It was proposed that the actin cross-linking function of β_H-

Spec could hold F-actin in place for the next cycle of myosin mediated-contraction, but this raises the question of how myosin and β_H-Spec association with F-actin are coordinated so that β_H-Spec prevents relaxation without interfering with constriction. Our results suggest a simple solution: since they compete for the same binding site, the release of myosin from F-actin at the end of a cycle of contraction would naturally be coupled to the accessibility of F-actin for binding by β_H-Spec. Thus the competition between myosin and β_H-Spec for binding to F-actin enables myosin-mediated cell contraction to effectively alternate with β_H-Spec-mediated stabilization.

Materials and methods

Drosophila genetics

Unless otherwise indicated, crosses were performed at 29°C. Protein localization and expression levels were monitored using previously characterized transgenes: *ex-lacZ* (Hamaratoglu et al., 2006), *kst:YFP* (Lye et al., 2014), *kst:GFP* (Nagarkar-Jaiswal et al., 2015), *jub:GFP* (Sabino et al., 2011), *sqh:GFP* (Royou et al., 2004), *sqh:mCherry* (Martin et al., 2009) and *β-Spec:GFP* (II) (this paper).

To manipulate gene expression in the posterior compartment, *en-Gal4 UAS-RFP; UAS-dcr2* flies were crossed with to UAS-RNAi or overexpression lines. RNAi transgenes used were *UAS-kstRNAi* (v37075), *UAS-kstRNAi* (HMS00882), *UAS-α-specRNAi* (v25387), *UAS-β-specRNAi* (GL01174), *UAS-rokRNAi* (v104675) and *UAS-jubRNAi* (v38442). To increase myosin activity, we used *UAS-sqh^{EE}*(Winter et al., 2001), and to increase β_H-Spec levels, we used *UAS-kstCRISPRa* (II) (this paper) and *UAS-kst$^{P[EPgy2]EY01010}$*(Pogodalla et al., 2021).

DNA Cloning

To overexpress β_H-Spec *(UAS-kstCRISPRa)*, we used a second-generation CRISPR/Cas9-transcriptional activation approach (Jia et al., 2018), allowing us to recruit the transcriptional machinery near the transcription start site (TSS) of *kst* under UAS control. For this, we made the following primers to generate a gRNA located less than 400 nt from the TSS: 5'-TTCGGATAAGCCGACAGGGTCTAT and 5'-AAACATAGACCCTGTCGGCTTATC-3' These primers were duplexed and cloned in the FlySAM 2.0 vector using the BbsI site (Jia et al., 2019). Transgenic flies were made by injection, inserting the construct into the attP40 site (BestGene).

The actin binding domain (aa 1-278) of *kst* was cloned into pGEX-3X at the EcoRI site, using the following primers: 5'-gatctgatcgaaggtcgtggaATGACCCAGCGGGACGGC-3' and 5'-atcgtcagtcagtcacgatgTTACTTCTTGCGATCTGCGTCCATTAGC-3', and assembled using NEBuilder® HiFi DNA Assembly (New England Biolabs, E2621) to generate plasmid pGEX-3X-ABDkst.

Recombineering was used to generate the β-Spec:GFP construct. A left homology arm (LHA, 1 kb before the stop codon of β-Spec) and a right homology arm (RHA, 1 kb after the stop codon of β-Spec) were cloned in pL452-cEGFP (Venken et al., 2008) by Gibson assembly into EcoRI (for LHA) and NotI (for RHA) sites, respectively, using the following primers: LHA_b-spec_FWD 5' gacctgcagccaagctatcgATACATGGCTGCCAAGGC 3'; LHA_b-spec_REV 5' gatcggaattgggctgcaggCTTTTTCTTTAAAGTAAAAAACGATCTGC 3'; RHA_b-spec_FWD 5' caagtaactagttctagagcAGTAACAGCCGTAACGCAAC 3' and RHA_b-spec_FWD 5' tggagctccaccgcggtggcCGGCAATTGGTGTACTTTAAAG 3'. The regions of the primers in lowercase indicate homology with the vector.

To activate the recombination machinery, SW106 E. coli containing the P[acman] clone CH322-20K3 (chloramphenicol resistant) (Venken et al., 2009) were incubated at 42°C for 17 min before making electrocompetent cells. A fragment containing LHA-loxP-NeoR/KanR-loxP-EGFP-RHA was amplified and electroporated into the cells. Recombinant clones were selected by chloramphenicol/kanamycin resistance and then floxed by inducible Cre expression by adding 0.1% L-arabinose. The final construct (LHA-loxP-EGFP-RHA) was confirmed by Sanger sequencing and injected for insertion in flies into the attP40 site (BestGene).

Histology and Imaging

For most experiments wing discs were fixed in 4% paraformaldehyde for 15 min at room temperature. Sqh:GFP discs were fixed for 12 min. Primary antibodies used were mouse anti-α-Spectrin (1:50, Developmental Studies Hybridoma Bank (DSHB), 3A9, deposited to the DSHB by Branton, D. / Dubreuil, R., RRID:AB_528473), rabbit anti-β-spectrin (1:100, a gift from Christian Klämbt) (Hulsmeier et al., 2007), rabbit anti-Dcr2 (1:800, Abcam, ab4732, RRID:AB_449344), rabbit anti-pMLC (T18/S19) (1:50, Cell Signaling Technologies, #3671, RRID:AB_330248), rat anti-E-cad (1:200, DSHB, DCAD2-c, deposited to the DSHB by Uemura, T., RRID:AB_528120), mouse β-galactosidase (1:200, DSHB, JIE7, deposited to the DSHB by Mason, T.L. / Partaledis, J.A., RRID:AB_528101). Secondary antibodies were used at a 1:100 dilution, and included anti-rat Alexa Fluor 647 (Jackson ImmunoResearch, 712-605-153, RRID:AB_2340694), anti-rabbit Alexa Flour 647 (Jackson ImmunoResearch, 711-605-152, RRID:AB_2492288), anti-mouse Alexa Fluor 647 (Jackson ImmunoResearch, 715-605-151, <colcnt=6> RRID:AB_2340863), anti-mouse Cy3 (Jackson ImmunoResearch, 715-165-151, RRID:AB_2315777), anti-rabbit Cy3 (Jackson ImmunoResearch, 711-165-152, RRID:AB_2307443), anti-rat Cy3 (Jackson ImmunoResearch, 712-165-153, RRID:AB_2340667), anti-mouse Alexa Fluor 488 (Thermo Fisher Scientific, A-21202, RRID:AB_141607) and anti-rabbit Alexa Flour 488 (Thermo Fisher Scientific, A-21206, RRID:AB_2535792). DNA was stained using Hoechst (Invitrogen, H3570). Wing discs were removed and mounted on a slide in Vectashield (Vector Laboratories, H-1000). Confocal images were captured on a Leica SP8 microscope.

Proximity Ligation Assay (PLA)

PLA was performed with the Duolink® Proximity Ligation Assay kit according to the manufacturer's instructions (Sigma). Fixation was performed as in the normal immunostaining procedure. For the permeabilization step, 0.5% Triton X-100 in PBS was used in two washes of 20 min each. Antibodies used for PLA include rabbit anti-GFP (1:200; ChromoTek # PABG1-20, RRID:AB_2749857)) and mouse α-Spectrin (1:50, Developmental Studies Hybridoma Bank, 3A9, RRID:AB_528473) antibodies, and secondary anti-mouse MINUS (Sigma-Aldrich Cat# DUO92004, RRID:AB_2713942) and anti-rabbit PLUS (Sigma-Aldrich Cat# DUO92002, RRID:AB_2810940) probes were used.

Immunoblotting

Wing discs (20 discs per lane) were lysed in 2× Laemmli Sample Buffer (Bio-Rad, #1610737) supplemented with protease inhibitor cocktail (Roche) and phosphatase inhibitor cocktail (Calbiochem). Protein samples were loaded in 4% to 15% gradient gels (Bio-Rad). Antibodies used for immunoblotting include mouse anti-GFP (1:1000; Cell Signaling Technology, #2955, RRID:AB_1196614) and as a loading control rabbit anti-GAPDH (1:5000; Santa Cruz Biotechnology, sc-25778, RRID:AB_10167668). Blots were visualized with fluorescent-

conjugated secondary antibodies (LI-COR Biosciences) and the Odyssey Imaging System (LICOR Biosciences).

Laser ablation

Live imaging and laser ablation experiments were performed as previously described (Rauskolb et al., 2014). *en-Gal4 UAS-RFP/CyO; UAS-dcr2/TM6B* flies were crossed with *UAS-kstRNAi; Ubi-E-cad:GFP/TM6B, UAS-a-specRNAi; Ubi-E-cad:GFP/TM6B* or *UAS-kstCRISPRa; Ubi-E-cad:GFP/TM6B* flies. Eggs were collected at 25°C for 4 hours and then shifted to 29°C for 88 h. Wing disc culture was based on the procedure of (Dye et al., 2017). A stock medium was prepared using Grace's medium (Sigma, G9771) without sodium bicarbonate but with the addition of 5 mM Bis-Tris and the pH was adjusted to 6.6-6.7 at room temperature. This was stored at 4°C for less than a month. Before every experiment, we added 5% fetal bovine serum (FBS; ThermoFisher, 10082147), Penicillin-Streptomycin (Thermo-Fisher, #15070063, 100X stock solution) and 10 nM 20-hydroxy-ecdysone (Sigma, H5142) to the medium. Larvae were floated on 25% sucrose and transferred into glass dishes with culture medium. Larvae of the desired genotype were selected and sterilized in 70% ethanol for 1 min. Then, we drew a circle on the glass bottom of a 35-mm glass-bottomed Petri dish (MatTek, P35G-0-14-C) using glue made by mixing heptane with tape (Tesa, 5388). Wing discs were dissected out of larvae, transferred into this Petri dish, and oriented using tungsten needles. Then we covered the discs with a Cyclopore Polycarbonate membrane (GE Health, 7060-2513) and glued it to the glass bottom to immobilize discs. Discs were imaged every 0.2 s on a Perkin Elmer Ultraview spinning disc confocal microscope, and ablation of junctions was achieved using a Micropoint pulsed laser (Andor Technology) tuned to 365 nm. Paired cutting of junctions, one in the anterior compartment and another in the posterior compartment at a similar location, were performed and compared. The displacement of vertices for the first second after ablation was used to calculate the velocities.

Quantification and Statistical Analysis

To obtain the surface of the wing disc and remove signals from the peripodial epithelium, we used the MATLAB toolbox ImSAnE (Heemskerk and Streichan, 2015) to detect and isolate a slice of the disc epithelium that surrounds the adherens junctions, using E-cad as a reference, as described previously (Pan et al., 2016). The KstGFP, KstYFP, SqhGFP and JubGFP images were created using ImSAnE.

For the fluorescence intensity heat maps, a custom MATLAB script was used (Alegot et al., 2019; Pan et al., 2018) (https://github.com/alegoth/Wing-disc-Intensity-Analysis). The script generates a 3D mask with the normalization channel (E-cad) keeping only the relevant pixels. The wing disc center (intersection between AP/DV boundaries) is picked for each image manually. Then, the picture is split into blocks of a given *xy* size (3×3 µm), starting from the center, and the average intensity per pixel of each channel is measured. The intensity of the reference channel and the channel of interest are normalized over their respective average intensity. The ratio of the channel of interest over the reference channel is then determined. To average several discs, only matrices of the same *xy* size blocks were used. The center of the disc serves as a reference point; smaller matrices were expanded to correspond to the size of the biggest matrix and filled with NaN (Not-a-Number). We determined the minimum number of values required (usually three) to average the ratio for a given position. This means that the edges of the average disk are composed of the same minimum number of values, which corresponds to the *n* given for each experiment. Finally, signals from several wing discs were averaged and represented by the heat map, and a posterior versus anterior ratio was calculated.

Pearson's correlation coefficient was calculated to establish co-localization between different proteins by using the Coloc 2 Plugin for ImageJ (https://imagej.net/plugins/coloc-2).

Statistical significance was determined with GraphPad Prism software by performing Student's t-test (for comparison between two observations) or analysis of variance (ANOVA) with $P<0.05$ set as the criteria for significance. The Dunnett test was used to derive adjusted P-values for comparisons against the control experimental value, and the Tukey test was used to derive adjusted P-values for multiple comparisons.

Protein production and purification

To purify the actin binding domain of β_H-Spec fused with GST, we transformed BL21-DE3 cells (NEB) with pGEX-3X-ABDkst. Protein expression was induced with 0.2 mM isopropyl-β-D-thiogalactoside (IPTG) at room temperature for 12–15 h. Cells were harvested and lysed by sonication in lysis buffer: PBS (pH 7.4), 1% Triton X-100, 5 mM dithiothreitol, 1 mM phenylmethyl sulfonyl fluoride and complete Mini Protease Inhibitor Cocktail (Roche). After centrifugation, the supernatant was collected and passed through a 1 mL GST-Trap column (Cytiva) at 4 °C. Then, the column was washed with PBS (pH 7.4) until the absorbance reached a steady baseline. To remove the GST-tag, the column was loaded with 80 units of Factor Xa (New England Biolabs, P8010) in cleavage buffer: 50 mM Tris-HCl, 150 mM NaCl, 1 mM $CaCl_2$, pH 7.5 and incubated for 16 h at room temperature. To elute the ABD of β_H-Spec while removing the protease simultaneously, we used a HiTrap Benzamidine FF (Cytiva) column in tandem with the GST-trap column and eluted the ABD of β_H-spec with cleavage buffer. To switch buffers, we dialyzed the protein against 25 mM HEPES pH 7.4, 150 mM NaCl, 1 mM TCP overnight. Then the purified protein was concentrated by ultrafiltration to 30 μM and stored at -80°C until used in experiments.

G-actin was prepared from rabbit muscle acetone powder as reported (Lehrer and Kerwar, 1972) and further purified with size exclusion chromatography on a Superdex 75 pg column (Cytiva, # 28989333) in buffer containing 5 mM Tris/HCl pH=8, 0.2 mM $CaCl_2$, 0.5 mM ATP, 1 mM DTT. G-actin was polymerized to F-actin by the addition of 10X polymerization buffer (100 mM HEPES pH 7.0, 500 mM KCl, 20 mM $MgCl_2$, 10 mM EDTA). *Drosophila* nonmuscle myosin-2 subfragment-1-like protein (*Zip*, amino acids 1-813) was recombinantly overproduced together with the myosin regulatory (*Sqh*) and essential light chain (*Mlc-c*) in the baculovirus/*Sf*9 insect cell system (Thermo Fisher Scientific) and prepared as described (Heissler et al., 2015).

Co-sedimentation assays

For co-sedimentation assays, β_H-Spec CH domains or myosin were incubated with F-actin for 15 mins at room temperature in an assay buffer containing 10 mM HEPES pH 7.4, 100 mM NaCl, 0.1 mM EGTA, 20μM ATP and 1 mM DTT and subsequently sedimented (100,000 x g, 15 min, 4°C, TLA-100 rotor) in an Ultima MAX-XP ultracentrifuge (Beckman). For competition assays, β_H-Spec and actin were preincubated for 15 mins at room temperature before the addition of myosin. Supernatant and pellet fractions were separated and the pellet fraction was resuspended in an equal volume of assay buffer. Samples were supplemented with NuPAGE LDS sample buffer (Invitrogen, #NP0007) and heated for 10 min at 90°C. Supernatant and pellet fractions were resolved on 4-12% NuPAGE Bis-Tris polyacrylamide gels (Invitrogen, NP0323BOX). Gels were incubated with PageBlue protein staining solution (Thermo Scientific, #24620) and destained with water. Gels were documented with a ChemiDoc MP (Bio-Rad) and densitometric analysis was performed with Fiji (Schindelin et al., 2012). Data plots and secondary analysis were performed in Origin 2019.

Model building

A homology model of the *Drosophila* myosin motor domain (*Zip*, amino acids 1-813) in the actin-bound state was modeled using the cryo-EM structure of the human nonmuscle myosin-2C motor domain in the rigor state (PDB entry: 5JLH) as a template. Both motor domains share ~ 72% sequence identity at the amino acid level. The motor domain model was built using Modeler (Sali and Blundell, 1993). The model of the *Drosophila* β_H-Spectrin calponin homology domain tandem (CH1-CH2, amino acids 1-278) was modeled using ColabFold (Mirdita et al., 2022). This model was superimposed onto the cryo-EM structure of the human β-III spectrin CH1 domain bound to F-actin (PDB entry: 6ANU) for binding site analysis.

Acknowledgements

We thank Christian Klämbt for the β-Spec antibody, and Richard Ebright and Bryce Nickels for sharing equipment for protein purification. This research was supported by National Institutes of Health grants GM131748 (KDI) and R01GM143539 (KC).

DATA and MATERIAL AVAILABILITY

All data generated or analyzed during this study are included in the manuscript and supporting files. All material including plasmids and transgenic fly lines generated in this study are available on request or through public repositories.

Figure Legends

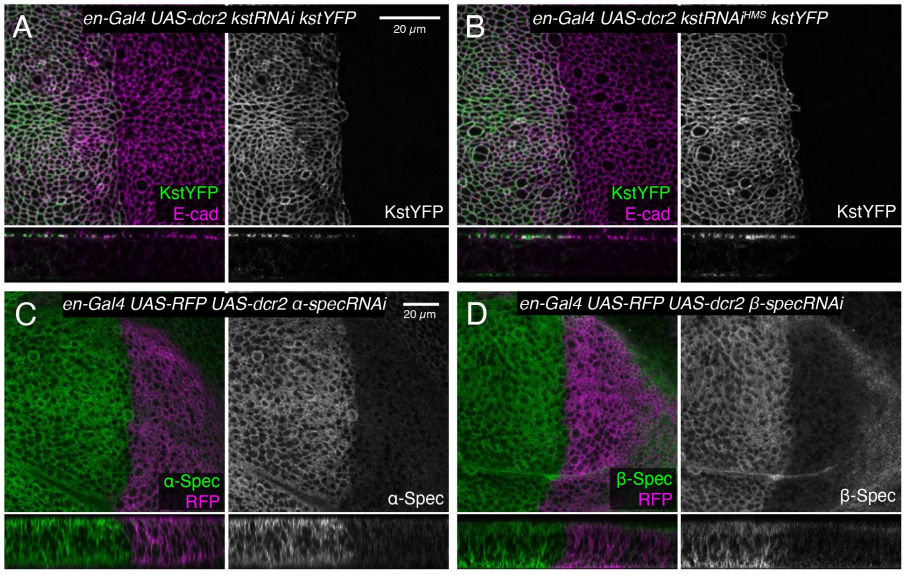

Figure 1 – figure supplement 1.

Validation of RNAi lines (A-B) horizontal (upper panels) and vertical (lower panels) sections of third instar wing imaginal discs expressing en-Gal4 UAS-dcr2 Kst:YFP (green/gray) crossed with UAS-kstRNAi(v37075) (A) and UAS-kstRNAi(HMS00882) (B), stained for E-cad (magenta). (C-D) Horizontal (upper panels) and vertical (lower panels) sections of third instar wing imaginal discs expressing en-Gal4 UAS-RFP (magenta) UAS-dcr2 crossed with UAS-α-specRNAi (C) or UAS-β-specRNAi (D) immunostained with α-Spec antibody or β-Spec antibody, respectively (green/gray). Gray scale images show the spectrin alone. β-specRNAi severely reduced β-Spec staining in most of the

wing disc but some signal remains near the peripodial membrane, which likely reflects non-specific staining by the antisera. Scale bar = 20 μm.

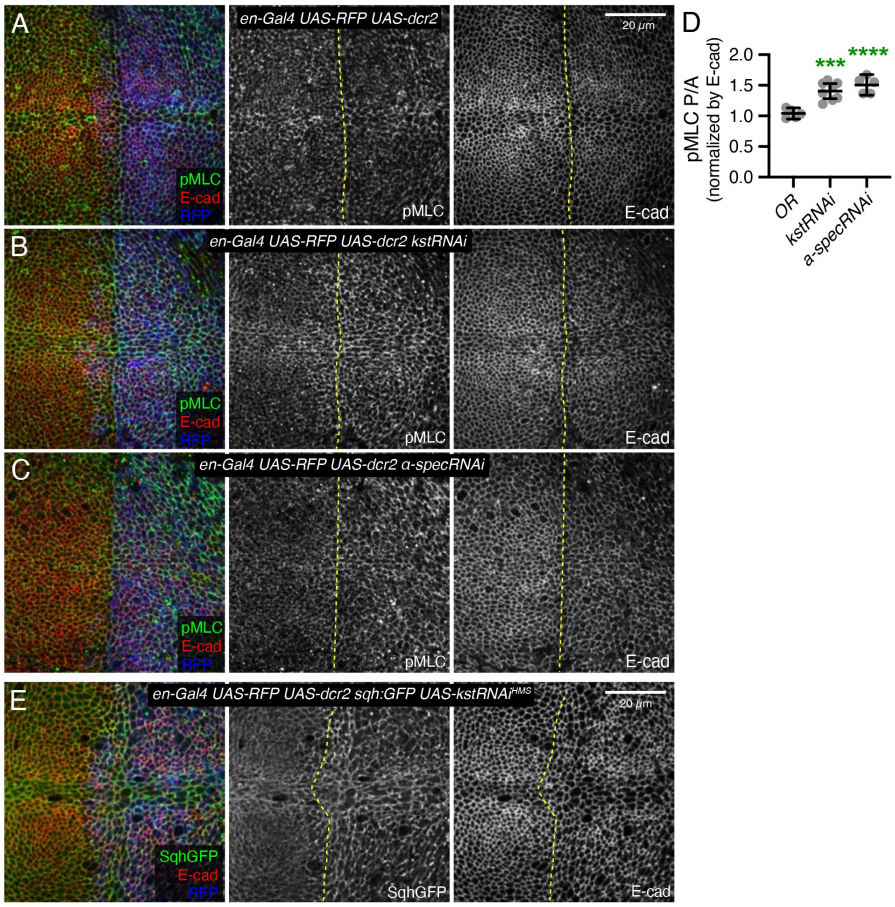

Figure 1 – figure supplement 2.

Modulation of levels of total and active myosin in wing discs by spectrins. (A-C) Apical sections of third instar wing imaginal discs expressing en-Gal4 UAS-dcr2 UAS-RFP (blue) crossed with control (A), UAS-kstRNAi(v37075) (B) and UAS-α-SpecRNAi (C), stained with pMLC antibody (green/gray) and E-cad (red/gray). (D) Quantification of pMLC normalized to E-cadherin in posterior cells (P) compared to anterior cells (A) in wing discs expressing the indicated constructs, displayed as individual values. Number of wing discs used for analysis: Control (OR), n=5; UAS-kstRNAi, n=8, UAS-α-SpecRNAi, n=5. Error bars show mean with 95% CI. Statistical significance was determined by one-way ANOVA with Dunnett's multiple comparison test. Statistical comparisons are shown relative to the control (OR). ***P≤0.001, ****P<0.0001. (E) Third instar wing imaginal discs expressing en-Gal4 UAS-dcr2 UAS-RFP (blue) sqh:GFP (green) in combination with UAS-kstRNAi(HMS00882). Panels to the right, in gray, show single channels, as indicated.

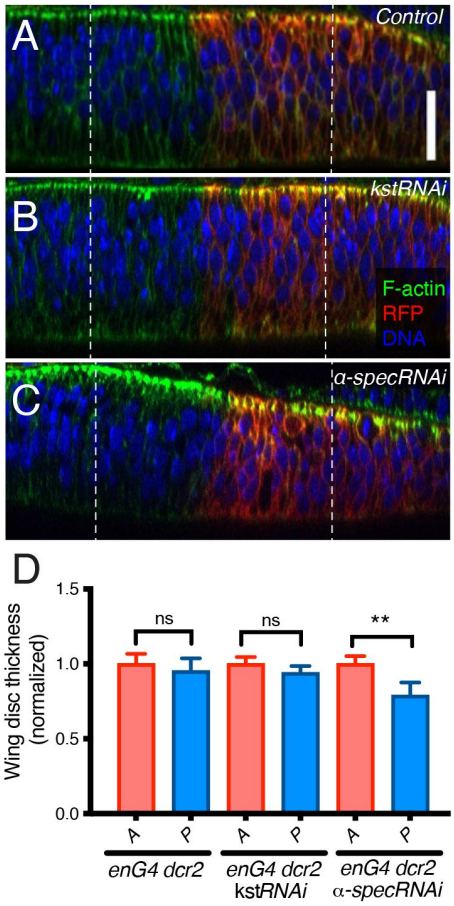

Figure 1 – figure supplement 3.

α-Spec knockdown decreases wing disc thickness. (A-C) Lateral views of wing discs expressing en-Gal4 UAS-RFP UAS-dcr2 crossed with control (Oregon-R, OR) (A), UAS-kstRNAi(v37075) (B) or UAS-α-specRNAi (C), stained with phalloidin to label F-actin (green), Hoechst to label nuclei (blue) and with the posterior compartment marked by RFP (red) and mounted with 40 µm spacers to avoid compressing the discs. Dashed lines indicate 30 µm from the A/P boundary. Scale bar = 20 µm (D) Quantification of wing imaginal disc thickness determined 30 µm from the A/P boundary in anterior (A) and posterior (P) sides for the different genotypes indicated. Statistical significance was determined by Student's t-test. ns: not significative; **P≤0.01; ***P≤0.001

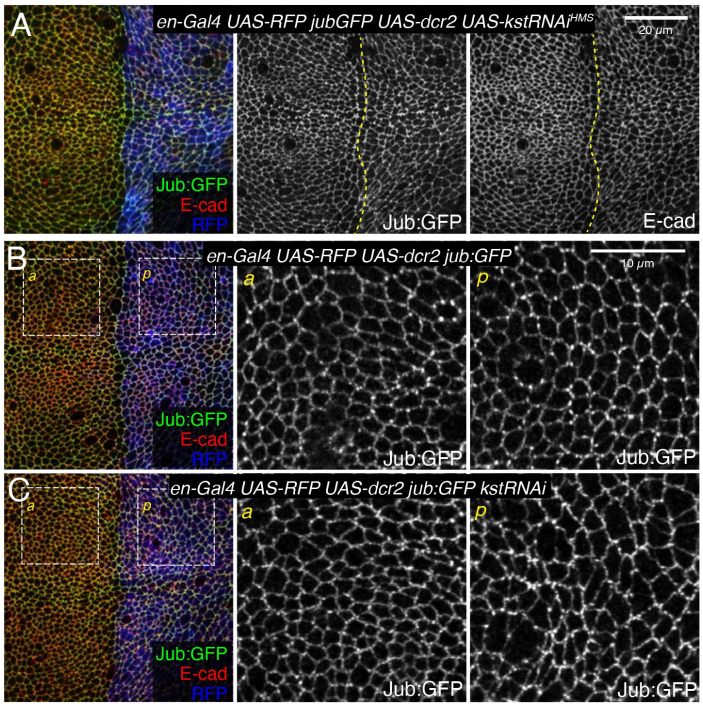

Figure 2 – figure supplement 1.

β_H-spec modulates the recruitment of Jub:GFP to AJs. (A) Third instar wing disc expressing en-Gal4 UAS-dcr2 UAS-RFP (blue) Jub:GFP (green/gray) in combination with UAS-kstRNAi(HMS00882) (A) stained for E-cad (red/gray). Dashed yellow line marks A/P compartment boundary. (B, C) Apical sections of wing discs expressing en-Gal4 UAS-RFP UAS-dcr2 Jub:GFP crossed to control (Oregon-R, OR) (B), UAS-kstRNAi(v37075) (C) from Figure 2. Columns to the right show higher magnification views of the Jub:GFP channel anterior (a) and posterior boxes (p).

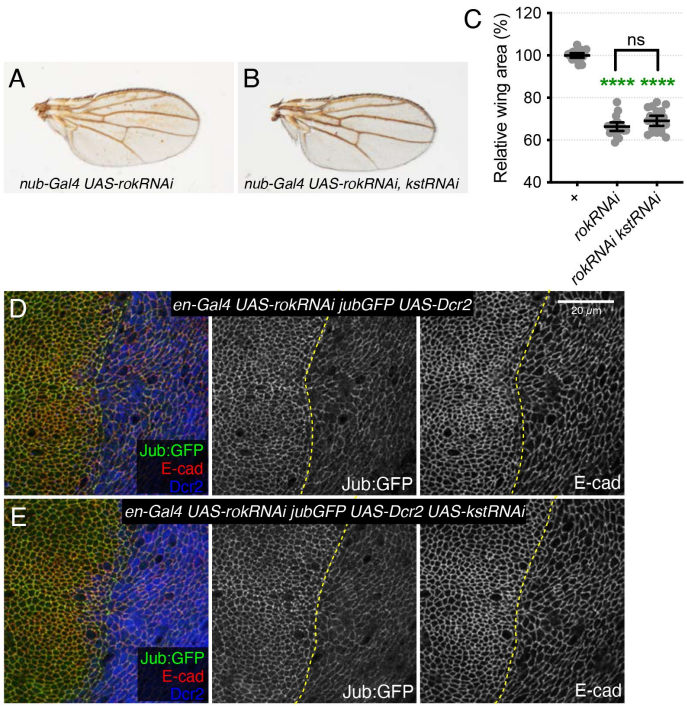

Figure 3 – figure supplement 1.

kst phenotypes are suppressed by reduction of tension (A-B) Representative adult wings from flies cultured at 29°C expressing nub-Gal4 and UAS transgenes reducing myosin activity (UAS-rokRNAi) enhancing RNAi (UAS-Dcr2) and in (B) knocking down β_H-Spec (UAS-kstRNAi(v37075)). (C) Quantification of wing area (mean and 95% CI, n = 20). Statistical significance was determined by one-way ANOVA with Tukey's multiple comparison test. Statistical comparisons are shown relative to nub-Gal4 UAS-dcr2 (data from Figure 3) in green or between nub-Gal4 UAS-dcr2 UAS-rokRNAi genotypes in black. (D-E) Sections of wing imaginal discs expressing en-Gal4 UAS-rokRNAi UAS-Dcr2 Jub:GFP crossed to control (Oregon-R) (D) or UAS-kstRNAi(v37075) (E) stained for E-cad (red/gray) showing the effect of reducing cytoskeletal tension on Jub:GFP (green/gray) in the posterior compartment (marked by Dcr2 immunostaining, blue). Scale bar = 20 µm.

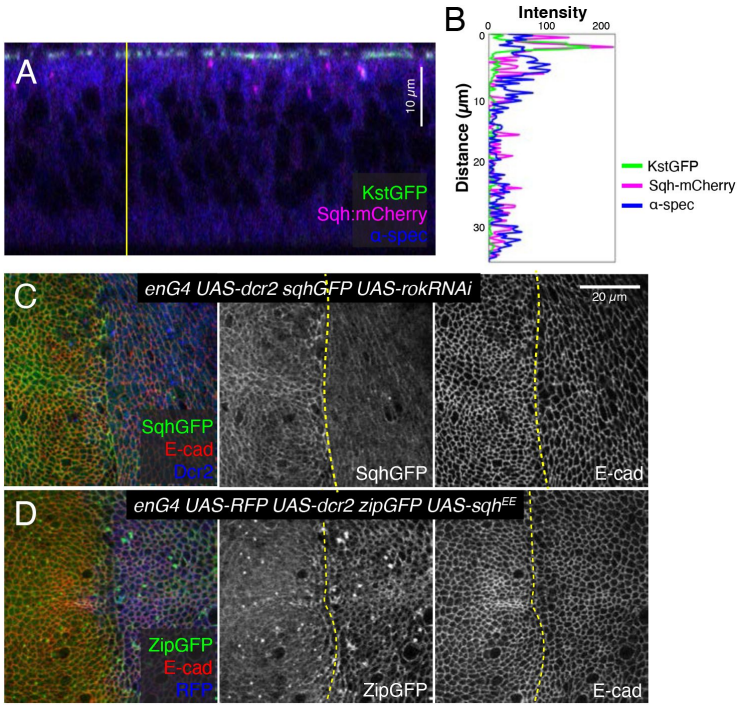

Figure 6 – figure supplement 1.

Additional analysis of β_H-Spec localization and the effect of changes in tension on myosin. (A) Lateral view of a wing imaginal disc co-expressing Kst:GFP (green) and the labelled myosin II subunit sqh:mCherry (magenta) stained with α-Spec antibody (blue). Scale bar = 10 µm (B) Linescan along the yellow line in A showing the intensities of Kst:GFP (green), Sqh::mCherry (magenta) and α-Spec. (C) Apical sections of a wing disc expressing en-Gal4 UAS-RFP UAS-dcr2 sqh:GFP crossed to UAS-rokRNAi in the posterior compartment (marked by Dcr2 immunostaining, blue), showing the effect of decreasing myosin activity on Sqh:GFP (green/gray). (D) Apical sections of a wing disc expressing en-Gal4 UAS-dcr2 zip:GFP (myosin heavy chain subunit tagged with GFP) crossed to UAS-sqh^{EE} in the posterior compartment (marked by RFP, blue), showing the effect of increasing myosin activity on Zip:GFP (green/gray). Discs were also stained for E-cad (red/gray). As described previously (Rauskolb et al., 2014), decreasing myosin activity decreases myosin levels near apical junctions and increasing myosin activity increases myosin levels near apical junctions. Scale bar = 20 µm.

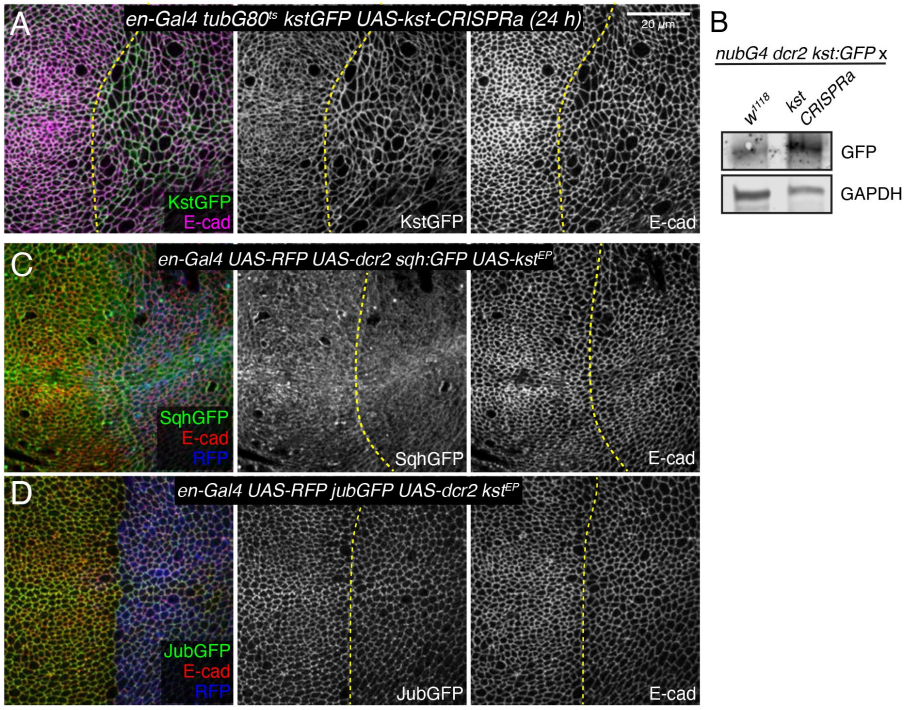

jub:GFP in combination with UAS-kstP[EPgy2] EY01010.

Figure 7 – figure supplement 1.

(A) Apical sections of a wing imaginal disc expressing en-Gal4 tubG80ts kst:GFP crossed with UAS-kst-CRISPRa, stained for E-cad (magenta). Expression of Kst:GFP (green) was induced by transferring the flies from 18°C to 29°C for 24 h. (B) Western blots of wing disc lysates with the genotypes shown in the figure: nub-Gal4 UAS-Dcr2 kst:GFP crossed with w^{1118} (control) and UAS-kstCRISPRa (experimental). Kst:GFP was detected using a GFP antibody. GAPDH was used as a loading control. (C) Third instar wing imaginal discs expressing enGal4 UAS-dcr2 UAS-RFP sqh:GFP in combination with UAS-kstP[EPgy2]EY01010. (D) Third instar wing imaginal discs expressing enGal4 UAS-dcr2 UAS-RFP

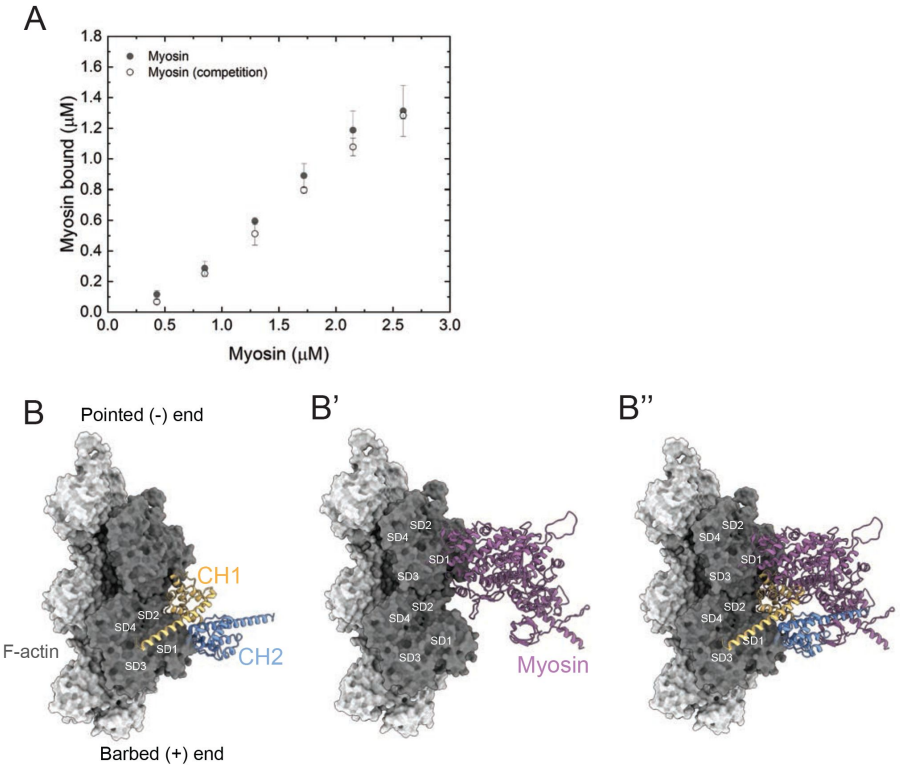

Figure 8 – figure supplement 1.

Additional examination of competition between β_H-Spec and myosin for F-actin. (A) Quantification of the binding behavior of myosin to F-actin in the presence and absence of spectrin in co-sedimentation assays. The similarity in actin binding indicates that pre-loading spectrin does not interfere with myosin binding to F-actin under these assay conditions. (B) Model of the *Drosophila* CH1-CH2 domain (CH1, yellow; CH2, blue) bound to F-actin (grey) (B'). Model of the *Drosophila* myosin motor domain (purple) bound to F-actin (grey) (B''). Superimposition of the CH1-CH2 and myosin motor domain on F-actin. The two strands of the actin filament are shown in light and dark grey and subdomains are indicated.

References

Alegot H. , Markosian C. , Rauskolb C. , Yang J. , Kirichenko E. , Wang Y. C. , Irvine K. D. (2019) **Recruitment of Jub by alpha-catenin promotes Yki activity and Drosophila wing growth** *J Cell Sci* **132**

Aragona M. , Panciera T. , Manfrin A. , Giulitti S. , Michielin F. , Elvassore N. , Dupont S. , Piccolo S (2013) **A mechanical checkpoint controls multicellular growth through YAP/TAZ regulation by actin-processing factors** *Cell* **154**:1047–1059

Avery A. W. , Crain J. , Thomas D. D. , Hays T. S (2016) **A human beta-III-spectrin spinocerebellar ataxia type 5 mutation causes high-affinity F-actin binding** *Sci Rep* **6**

Avery A. W. , Fealey M. E. , Wang F. , Orlova A. , Thompson A. R. , Thomas D. D. , Hays T. S. , Egelman E. H. (2017) **Structural basis for high-affinity actin binding revealed by a beta-III-spectrin SCA5 missense mutation** *Nat Commun* **8**

Das Thakur M. , Feng Y. , Jagannathan R. , Seppa M. J. , Skeath J. B. , Longmore G. D. (2010) **Ajuba LIM proteins are negative regulators of the Hippo signaling pathway** *Curr Biol* **20**:657–662

Deng H. , Wang W. , Yu J. , Zheng Y. , Qing Y. , Pan D (2015) **Spectrin regulates Hippo signaling by modulating cortical actomyosin activity** *Elife* **4**

Deng H. , Yang L. , Wen P. , Lei H. , Blount P. , Pan D (2020) **Spectrin couples cell shape, cortical tension, and Hippo signaling in retinal epithelial morphogenesis** *J Cell Biol* **219**

Dietzl G. , Chen D. , Schnorrer F. , Su K. C. , Barinova Y. , Fellner M. , Gasser B. , Kinsey K. , Oppel S. , Scheiblauer S. , et al. (2007) **A genome-wide transgenic RNAi library for conditional gene inactivation in Drosophila** *Nature* **448**:151–156

Duan R. , Kim J. H. , Shilagardi K. , Schiffhauer E. S. , Lee D. M. , Son S. , Li S. , Thomas C. , Luo T. , Fletcher D. A. , et al. (2018) **Spectrin is a mechanoresponsive protein shaping fusogenic synapse architecture during myoblast fusion** *Nat Cell Biol* **20**:688–698

Dubreuil R. , Byers T. J. , Branton D. , Goldstein L. S. , Kiehart D. P (1987) **Drosophilia spectrin** *I. Characterization of the purified protein. J Cell Biol* **105**:2095–2102

Dubreuil R. R. , Maddux P. B. , Grushko T. A. , MacVicar G. R (1997) **Segregation of two spectrin isoforms: polarized membrane-binding sites direct polarized membrane skeleton assembly** *Mol Biol Cell* **8**:1933–1942

Dye N. A. , Popovic M. , Spannl S. , Etournay R. , Kainmuller D. , Ghosh S. , Myers E. W. , Julicher F. , Eaton S (2017) **Cell dynamics underlying oriented growth of the Drosophila wing imaginal disc** *Development* **144**:4406–4421

Fernandez B. G. , Gaspar P. , Bras-Pereira C. , Jezowska B. , Rebelo S. R. , Janody F (2011) **Actin-Capping Protein and the Hippo pathway regulate F-actin and tissue growth in Drosophila** *Development* **138**:2337–2346

Fernandez-Gonzalez R. , Simoes S. d. M. , Röper J.-C. , Eaton S. , Zallen J. A. (2009) **Myosin II dynamics are regulated by tension in intercalating cells** *Developmental Cell* **17**:736–743

Fletcher G. C. , Elbediwy A. , Khanal I. , Ribeiro P. S. , Tapon N. , Thompson B. J (2015) **The Spectrin cytoskeleton regulates the Hippo signalling pathway** *EMBO J* **34**:940–954

Forest E. , Logeay R. , Geminard C. , Kantar D. , Frayssinoux F. , Heron-Milhavet L. , Djiane A (2018) **The apical scaffold big bang binds to spectrins and regulates the growth of Drosophila melanogaster wing discs** *J Cell Biol* **217**:1047–1062

Greenberg M. J. , Arpag G. , Tuzel E. , Ostap E. M (2016) **A Perspective on the Role of Myosins as Mechanosensors** *Biophys J* **110**:2568–2576

Hamaratoglu F. , Willecke M. , Kango-Singh M. , Nolo R. , Hyun E. , Tao C. , Jafar-Nejad H. , Halder G. (2006) **The tumour-suppressor genes NF2/Merlin and Expanded act through Hippo signalling to regulate cell proliferation and apoptosis** *Nat Cell Biol* **8**:27–36

Heemskerk I. , Streichan S. J (2015) **Tissue cartography: compressing bio-image data by dimensional reduction** *Nat Methods* **12**:1139–1142

Heissler S. M. , Chinthalapudi K. , Sellers J. R (2015) **Kinetic characterization of the sole nonmuscle myosin-2 from the model organism Drosophila melanogaster** *FASEB J* **29**:1456–1466

Heissler S. M. , Manstein D. J (2013) **Nonmuscle myosin-2: mix and match** *Cell Mol Life Sci* **70**:1–21

Hulsmeier J. , Pielage J. , Rickert C. , Technau G. M. , Klambt C. , Stork T (2007) **Distinct functions of alpha-Spectrin and beta-Spectrin during axonal pathfinding** *Development* **134**:713–722

Ibar C. , Kirichenko E. , Keepers B. , Enners E. , Fleisch K. , Irvine K. D (2018) **Tension-dependent regulation of mammalian Hippo signaling through LIMD1** *J Cell Science* **131**

Jia Y. , Shen D. , Wang X. , Sun J. , Peng P. , Xu R. G. , Xu B. , Ni J. Q (2019) **flySAM Transgenic CRISPRa System Manual** *Bio Protoc* **9**

Jia Y. , Xu R. G. , Ren X. , Ewen-Campen B. , Rajakumar R. , Zirin J. , Yang-Zhou D. , Zhu R. , Wang F. , Mao D. , et al. (2018) **Next-generation CRISPR/Cas9 transcriptional activation in Drosophila using flySAM** *Proc Natl Acad Sci U S A* **115**:4719–4724

Khanna M. R. , Mattie F. J. , Browder K. C. , Radyk M. D. , Crilly S. E. , Bakerink K. J. , Harper S. L. , Speicher D. W. , Thomas G. H (2015) **Spectrin tetramer formation is not required for viable development in Drosophila** *J Biol Chem* **290**:706–715

Kiehart D. P. , Feghali R (1986) **Cytoplasmic myosin from Drosophila melanogaster** *J Cell Biol* **103**:1517–1525

Krueger D. , Pallares Cartes C. , Makaske T. , De Renzis S. (2020) **betaH-spectrin is required for ratcheting apical pulsatile constrictions during tissue invagination** *EMBO Rep* **21**

Lee J. K. , Brandin E. , Branton D. , Goldstein L. S (1997) **alpha-Spectrin is required for ovarian follicle monolayer integrity in Drosophila melanogaster** *Development* **124**:353–362

Lehrer S. S. , Kerwar G (1972) **Intrinsic fluorescence of actin** *Biochemistry* **11**:1211–1217

Liem R. K (2016) **Cytoskeletal Integrators: The Spectrin Superfamily** *Cold Spring Harb Perspect Biol* **8**

Lye C. M. , Naylor H. W. , Sanson B (2014) **Subcellular localisations of the CPTI collection of YFP-tagged proteins in Drosophila embryos** *Development* **141**:4006–4017

Machnicka B. , Czogalla A. , Hryniewicz-Jankowska A. , Boguslawska D. M. , Grochowalska R. , Heger E. , Sikorski A. F (2014) **Spectrins: a structural platform for stabilization and activation of membrane channels, receptors and transporters** *Biochim Biophys Acta* **1838**:620–634

Martin A. C. , Kaschube M. , Wieschaus E. F (2009) **Pulsed contractions of an actin-myosin network drive apical constriction** *Nature* **457**:495–499

Mirdita M. , Schutze K. , Moriwaki Y. , Heo L. , Ovchinnikov S. , Steinegger M (2022) **ColabFold: making protein folding accessible to all** *Nat Methods* **19**:679–682

Misra J. R. , Irvine K. D (2018) **The Hippo Signaling Network and its Biological Functions** *Annual Reviews of Genetics* **52**

Nagarkar-Jaiswal S. , Lee P. T. , Campbell M. E. , Chen K. , Anguiano-Zarate S. , Gutierrez M. C. , Busby T. , Lin W. W. , He Y. , Schulze K. L. , et al. (2015) **A library of MiMICs allows tagging of genes and reversible, spatial and temporal knockdown of proteins in Drosophila** *Elife* **4**

Noll N. , Mani M. , Heemskerk I. , Streichan S. J. , Shraiman B. I (2017) **Active tension network model suggests an exotic mechanical state realized in epithelial tissues** *Nature Physics* **13**:1221–1226

Pan Y. , Alegot H. , Rauskolb C. , Irvine K. D (2018) **The dynamics of Hippo signaling during Drosophila wing development** *Development* **145**

Pan Y. , Heemskerk I. , Ibar C. , Shraiman B. I. , Irvine K. D (2016) **Differential growth triggers mechanical feedback that elevates Hippo signaling** *Proc Natl Acad Sci U S A* **113**:E6974–E6983

Papal S. , Cortese M. , Legendre K. , Sorusch N. , Dragavon J. , Sahly I. , Shorte S. , Wolfrum U. , Petit C. , El-Amraoui A (2013) **The giant spectrin betaV couples the molecular motors to phototransduction and Usher syndrome type I proteins along their trafficking route** *Hum Mol Genet* **22**:3773–3788

Pogodalla N. , Kranenburg H. , Rey S. , Rodrigues S. , Cardona A. , Klambt C (2021) **Drosophila ssHeavy-Spectrin is required in polarized ensheathing glia that form a diffusion-barrier around the neuropil** *Nat Commun* **12**

Rauskolb C. , Cervantes E. , Madere F. , Irvine K. D (2019) **Organization and function of tension-dependent complexes at adherens junctions** *J Cell Sci* **132**

Rauskolb C. , Han A. , Kirichenko E. , Ibar C. , Irvine K. D (2022) **Analysis of the Drosophila Ajuba LIM protein defines functions for distinct LIM domains** *PLoS One* **17**

Rauskolb C. , Pan G. , Reddy B. V. , Oh H. , Irvine K. D (2011) **Zyxin links fat signaling to the hippo pathway** *PLoS Biol* **9**

Rauskolb C. , Sun S. , Sun G. , Pan Y. , Irvine K. D (2014) **Cytoskeletal tension inhibits Hippo signaling through an Ajuba-Warts complex** *Cell* **158**:143–156

Razzell W. , Bustillo M. E. , Zallen J. A (2018) **The force-sensitive protein Ajuba regulates cell adhesion during epithelial morphogenesis** *J Cell Biol, jcb* **201801171**

Royou A. , Field C. , Sisson J. C. , Sullivan W. , Karess R (2004) **Reassessing the role and dynamics of nonmuscle myosin II during furrow formation in early Drosophila embryos** *Mol Biol Cell* **15**:838–850

Sabino D. , Brown N. H. , Basto R (2011) **Drosophila Ajuba is not an Aurora-A activator but is required to maintain Aurora-A at the centrosome** *J Cell Sci* **124**:1156–1166

Sali A. , Blundell T. L (1993) **Comparative protein modelling by satisfaction of spatial restraints** *J Mol Biol* **234**:779–815

Sansores-Garcia L. , Bossuyt W. , Wada K. , Yonemura S. , Tao C. , Sasaki H. , Halder G. (2011) **Modulating F-actin organization induces organ growth by affecting the Hippo pathway** *EMBO J* **30**:2325–2335

Sarpal R. , Yan V. , Kazakova L. , Sheppard L. , Yu J. C. , Fernandez-Gonzalez R. , Tepass U (2019) **Role of α-Catenin and its mechanosensing properties in regulating Hippo/YAP-dependent tissue growth** *PLoS Genet* **15**

Schindelin J. , Arganda-Carreras I. , Frise E. , Kaynig V. , Longair M. , Pietzsch T. , Preibisch S. , Rueden C. , Saalfeld S. , Schmid B. , et al. (2012) **Fiji: an open-source platform for biological-image analysis** *Nat Methods* **9**:676–682

Sellers J. R. , Eisenberg E. , Adelstein R. S (1982) **The binding of smooth muscle heavy meromyosin to actin in the presence of ATP. Effect of phosphorylation** *J Biol Chem* **257**:13880–13883

Sun S. , Reddy B. V. , Irvine K. D (2015) **Localization of Hippo signalling complexes and Warts activation in vivo** *Nat Commun* **6**

Thomas G. H. , Kiehart D. P (1994) **Beta heavy-spectrin has a restricted tissue and subcellular distribution during Drosophila embryogenesis** *Development* **120**:2039–2050

Thomas G. H. , Zarnescu D. C. , Juedes A. E. , Bales M. A. , Londergan A. , Korte C. C. , Kiehart D. P (1998) **Drosophila betaHeavy-spectrin is essential for development and contributes to specific cell fates in the eye** *Development* **125**:2125–2134

Vasquez C. G. , Heissler S. M. , Billington N. , Sellers J. R. , Martin A. C (2016) **Drosophila non-muscle myosin II motor activity determines the rate of tissue folding** *Elife* **5**

Venken K. J. , Carlson J. W. , Schulze K. L. , Pan H. , He Y. , Spokony R. , Wan K. H. , Koriabine M. , de Jong P. J. , White K. P. , et al. (2009) **Versatile P[acman] BAC libraries for transgenesis studies in Drosophila melanogaster** *Nat Methods* **6**:431–434

Venken K. J. , Kasprowicz J. , Kuenen S. , Yan J. , Hassan B. A. , Verstreken P (2008) **Recombineering-mediated tagging of Drosophila genomic constructs for in vivo localization and acute protein inactivation** *Nucleic Acids Res* **36**

von der Ecken J. , Heissler S. M. , Pathan-Chhatbar S. , Manstein D. J. , Raunser S. (2016) **Cryo-EM structure of a human cytoplasmic actomyosin complex at near-atomic resolution** *Nature* **534**:724–728

Winter C. G. , Wang B. , Ballew A. , Royou A. , Karess R. , Axelrod J. D. , Luo L (2001) **Drosophila Rho-associated kinase (Drok) links Frizzled-mediated planar cell polarity signaling to the actin cytoskeleton** *Cell* **105**:81–91

Wong K. K. , Li W. , An Y. , Duan Y. , Li Z. , Kang Y. , Yan Y (2015) **beta-Spectrin regulates the hippo signaling pathway and modulates the basal actin network** *J Biol Chem* **290**:6397–6407

Xie S. , Martin A. C (2015) **Intracellular signalling and intercellular coupling coordinate heterogeneous contractile events to facilitate tissue folding** *Nat Commun* **6**

Zarnescu D. C. , Thomas G. H (1999) **Apical spectrin is essential for epithelial morphogenesis but not apicobasal polarity in Drosophila** *J Cell Biol* **146**:1075–1086

Zheng Y. , Pan D (2019) **The Hippo Signaling Pathway in Development and Disease** *Dev Cell* **50**:264–282

Author information

Consuelo Ibar
Waksman Institute and Department of Molecular Biology and Biochemistry, Rutgers University, Piscataway NJ 08854 USA
ORCID iD: 0000-0002-1965-2696

Krishna Chinthalapudi
Department of Physiology and Cell Biology, Dorothy M. Davis Heart and Lung Research Institute, The Ohio State University College of Medicine, Columbus, Ohio, USA
ORCID iD: 0000-0003-3669-561X

Sarah M. Heissler
Department of Physiology and Cell Biology, Dorothy M. Davis Heart and Lung Research Institute, The Ohio State University College of Medicine, Columbus, Ohio, USA

Kenneth D. Irvine
Waksman Institute and Department of Molecular Biology and Biochemistry, Rutgers University, Piscataway NJ 08854 USA
For correspondence: irvine@waksman.rutgers.edu
ORCID iD: 0000-0002-0515-3562

Editors

Reviewing Editor
Michael Eisen
University of California, Berkeley, United States of America

Senior Editor
Michael Eisen
University of California, Berkeley, United States of America

Reviewer #1 (Public Review):

Ibar and colleagues investigate the function of spectrin in Drosophila wing imaginal discs and its effect on the Hippo pathway and myosin activity. The authors find that both βH-Spec and its canonical binding partner α-Spec reduce junctional localization of the protein Jub and thereby restrict Jub's inhibitory effect on Hippo signaling resulting in activation of the Hippo effector Yorkie regulating tissue shape and organ size. From genetic epistasis analysis and analysis of protein localization, the authors conclude that βH-Spec and α-Spec act independently in this regulation. The major point of this study is that the apical localization of βH-Spec and myosin is mutually exclusive and that the proteins antagonize each other's activity in wing discs. In vitro co-sedimentation assays and in silico structural modeling suggest that this antagonization is due to a competition of βH-Spec and myosin for F-actin binding.

The study's strengths are the genetic perturbation that is the basis for the epistasis analysis which includes specific knockdowns of the genes of interest as well as an elegant CRISPR-

based overexpression system with great tissue specificity. The choice of the model for such an in-depth analysis of pathway dependencies in a well-characterized tissue makes it possible to identify and characterize quantitative differences between closely entangled and mutually dependent components. The method of quantifying protein localization and abundance is common for multiple figures which makes it easy to assess differences across experiments. The flow of experiments is logical and in general, the author's conclusions are supported by the presented data. The findings are very well embedded into the context of relevant literature and both confronting and confirming literature are discussed.

The study shows how components of the cytoskeleton are directly involved in the regulation of the mechanosensitive Hippo pathway in vivo and thus ultimately regulate organ size supporting previous data in other contexts. The molecular mechanism regulating myosin activity by out-competing it for F-actin binding has been observed for small actin-binding proteins such as cofilin but is a new mode for such a big, membrane-associated actin-binding protein. This may inspire future experiments in different morphogenetic contexts for the investigation of similar mechanisms. For example, the antagonistic activity of βH-Spec and myosin in this tissue context might help explain phenomena in other systems such as spectrin-dependent ratcheting of apical constriction during mesoderm invagination (as the authors discuss). Against the classical view, the work shows that βH-Spec can act independently of α-Spec. Together the results will be of interest to the cell biology community with a focus on the cytoskeleton and mechanotransduction.

Reviewer #2 (Public Review):

Ibar and colleagues address the role of the spectrin cytoskeleton in the regulation of tissue growth and Hippo signaling in an attempt to elucidate the underlying molecular mechanism(s) and reconcile existing data. Previous reports in the field have suggested three distinct mechanisms by which the Spectrin cytoskeleton regulates Hippo signaling and this is, at least in part, due to the fact that different groups have mainly focused on different spectrins (alpha, beta, or beta-heavy) in previous reports.

The authors start their investigation by trying to reconcile their previous data on the role of Ajuba in the regulation of Hippo signaling via mechanotransduction and previous observations suggesting that Spectrins affect Hippo signaling independently of any effect on myosin levels or Ajuba localization. Contrary to previous reports, the authors reveal that, indeed, depletion of alpha- and beta-heavy-spectrin leads to an increase in myosin levels at the apical membrane. Moreover, the authors also reveal that the depletion of spectrins leads to an increase in Ajuba levels.

Author Response:

The following is the authors' response to the original reviews.

We thank both reviewers for their comments, which have suggested changes that have improved the manuscript.

> ***Reviewer #1 (Public Review):***
>
> *[…] A weakness in the methodology is the link to tissue tension and conclusions about tissue mechanics. Methods that directly affect tissue tension and a more thorough and systematic application of laser ablation experiments would be needed to profoundly investigate mechanosensation and consequential effects on tissue tension by the various genetic perturbations.*

Response: In revision, we have added some additional experiments that examine altered tension.

> *While the in-silico analysis of competing for F-actin binding sites for βH-Spec and myosin appears logical and supports the authors' claims, no point mutation or truncations were used to test these results in vivo.*
>
> *In its current structure the manuscript's strength, the genetic perturbations, is compromised by missing clear assessments of knockdown efficiencies early in the manuscript and other controls such as the actual effect on myosin by ROCK overactivation.*

Response: In revision, we reorganized the manuscript and figures to document the knockdown efficiency earlier in the manuscript, and have added additional figure panels illustrating the effects of altered tension on myosin levels.

> ***Reviewer #2 (Public Review):***
>
> *[…] The authors suggest that Ajuba is required for the effect of beta-heavy spectrin. However, it is still formally possible that this could be a parallel pathway that is being masked by the strong phenotype of Ajuba RNAi flies.*

Response: While it is formally true that the genetic requirement for Jub could reflect a role in parallel to, rather than downstream of, spectrins, our conclusion that spectrins act through Jub is based not only on the genetic requirement for Jub, but also on the influence of spectrins on junctional tension and Jub localization, which indicate that spectrins influence Jub activity in a manner consistent with their affecting the Hippo pathway through Jub.

> *One of the major points of the manuscript is the observation that alpha- and beta-heavy-spectrin are potentially working independently and not as part of a spectrin tetramer. This is mostly dependent on the observation that alpha- and beta-heavy-spectrin appear to have non-overlapping localizations at the membrane and the fact that alpha- and beta-heavy-spectrin localize at the membrane seemingly independently. It is not entirely obvious that a potential lack of colocalization and the fact that protein localization at the membrane is not affected when the other partner is absent is sufficient to argue that alpha- and beta-heavy-spectrin do not form a complex. Moreover, it is possible that the spectrin complexes are only formed in specific conditions (e.g. by modulating tissue tension).*

Response: Our results argue that alpha- and beta-heavy-spectrin do not form a detectable complex in the wing disc under the conditions examined, and thus that they act independently is this context. However, we agree that it is possible that they could function together contexts, eg in other tissues or under different conditions, and we have revised the text in the Discussion to note this.

> *If indeed spectrins function independently, would it not be expected to see additive effects when both spectrins are depleted?*

Response: Not necessarily, since both alpha- and beta-heavy-spectrin act through Jub, and there may be a limit as to how much Yki activity can be increased by Jub (eg the increases in wing size induced by spectrin RNAi are similar to the increases in wing size observed with constitutive recruitment of Jub through alpha-catenin mutation (Alegot et al 2019).

> *Related to the two previous points, the fact that the authors suggest that both alpha- and beta-heavy-spectrin regulate Hippo signaling via Ajuba would be consistent with the necessity of an alpha- and beta-heavy-spectrin complex being formed. How would the authors explain that both spectrins require Ajuba function but work independently?*

Response: The different spectrins both affect Jub because they both affect cytoskeletal tension, but our results suggest that they act in different ways to affect tension. We have made some revisions to the Discussion section to try to make this clearer.

> *Another major point of the manuscript is the potential competition between beta-heavy-spectrin and myosin for F-actin binding. The authors suggest that there is a mutual antagonism between the two proteins regarding apical F-actin. However, this has not been formally assessed. Moreover, despite the arguments put forward in the discussion, it seems hard to justify a competition for F-actin when beta-heavy-spectrin seems to be unable to compete with myosin. Myosin can displace beta-heavy-spectrin from F-actin but the reciprocal effect seems unlikely given the in vitro data.*

Response: We show in vivo, in vitro, and in silico data that are all consistent with the inference that beta-heavy-spectrin and myosin compete for binding to F-actin. As the reviewer notes, and as we discuss, the in vitro competition experiments were limited because, for technical reason, we were unable to increase the protein concentrations higher. We also note that our in vitro experiments used an active form of myosin, which binds F-actin much more strongly than inactive myosin.

> ***Reviewer #1 (Recommendations For The Authors):***
>
> *While the flow of experiments is logical in general, I see major problems regarding the structure of the manuscript and essential controls:*
>
> *It is very confusing to have samples (kst-CRISPRa) in figures 1-3 that were not introduced in the text until the second-last paragraph of the results. I would suggest introducing this elegant overexpression experiment early in the manuscript as it fits well in the scope of these experiments or alternatively (if the authors prefer) make a new figure containing all the data regarding the overexpression in the end.*

Response: We have now moved these results to a new figure (new Fig 7) that is described later in the text.

> *• At the beginning of the manuscript, essential controls regarding the knockdown efficiency are missing in the main figure. Many of the key experiments are based on KD and as a reader, I want to assess their efficiency. Only in Figure 4, at the end of the manuscript, KST and α-Spec KD efficiency is revealed - this should be shown earlier and quantified properly. While reading the manuscript in its current form, the doubt remains that differences e.g. in α-Spec and KST KD can be explained by varying knockdown efficiencies as their levels can't be assessed.*

Response: We have now moved these results to a new supplemental figure (Fig 1-supplement 1) that is cited earlier in the text.

> *• On a similar line, in Figure 5 where myosin activity is perturbed, induction or repression of myosin activity is only suggested but not formally shown. The authors have to demonstrate that this is indeed the case by showing the myosin signal, ideally accompanied by measurement of tissue tension.*

Response: This was not included because we and others have assessed these manipulations in earlier publications. However, as requested we have now added a supplemental figure (Fig 6 supplement 1) showing myosin levels in these genotypes.

> *• On p. 7, the authors claim that "The epistasis of jub to kst suggests that βH-Spec regulates wing size through its tension-dependent regulation of Jub." While the authors show that KST KD increases myosin and junctional Jub, and that the wing overgrowth phenotype of KST KD depends on Jub, the tension-dependency was not demonstrated. To make that claim, the tension profile should be perturbed e.g. by overexpression of rok, myosin mutants (as the authors do in Fig 5) and the effect on Jub should be analyzed. Induction of tension in these conditions should be measured by laser ablation or a suitable alternative method. It might well be that the induction of Jub in KST KD is not via tension but an alternative mechanism such as the release of steric hindrance, interaction competition, etc. Also: Does KD of Jub affect spectrin localization?*

Response: The effect of tension on Jub, and the effects of the myosin activity changes we employed on tension, have been analyzed in prior publications (eg Rauskolb et al 2014). To further address the issue raised by the reviewer here as to whether Kst affects Jub and wing growth via tension, we have also now added an additional experiment (Fig 3 supplement 1) in which we decreased tension in a βH-Spec RNAi wing disc by simultaneously expressing RNAi targeting Rok. The results show that the wing growth and Jub accumulation associated with βH-Spec RNAi are suppressed by Rok RNAi, consistent with our conclusion that these effects are mediated via cytoskeletal tension.

As KD of Jub alters the pattern of myosin accumulation in wing discs (Rauskolb et al 2019) it could be expected to have a complementary influence on βH-Spec localization, but we have not examined this.

> *• The authors make a very strong point in saying "The influence of βH-Spec on junctional tension is thus a direct consequence of its competition with myosin for overlapping binding sites on F-actin." While the authors provide some in vitro and in silico evidence, it was for example not possible to outcompete myosin by increasing levels of KST CH1-CH2 domains in vitro (for possible reasons the authors discuss). More importantly, the hypothesis that competition for actin binding is the definite cause of the antagonizing effect was not tested in vivo. Overexpression of a mutant version of KST that is unable to bind F-actin, or that has an increased affinity (etc) for actin was not tested. Such an experiment would be very valuable to enrich this manuscript but at least, claims like that have to be less bold and need to be written in a more speculative language.*

Response: We consider creating and analyzing mutant forms of Kst in vivo to be beyond the scope of this manuscript, but as suggested we have now modified the text highlighted by the Reviewer to be more cautious.

> *Further points:*
>
> *• Why does the thickness of the wing disc epithelium change due to KST and α Spec KD, the authors should introduce this experiment better and draw a proper conclusion. Is there any relocalization of myosin along the apical-basal axis? Can the authors speculate about the differences between KST and α Spec KD?*

Response: The epithelium thickness changes with α-Spec KD, but does not change with Kst KD. We think the explanation is provided by work from the Pan lab (done mainly in pupal

eyes), which reported decreased cortical tension and increased apical area when α-Spec is lost. The interpretation in essence is that with the loss of attachment of F-actin to membranes along the lateral sides of the cells, the sides of the cells are "softer" and the cells expand laterally and thus also (by conservation of volume) shorten apical-basally. This is somewhat speculative, and it's not a focus of our study, but we have added some text to try to explain this better. Myosin along apical-basal axis was not visibly altered, but it is harder to analyze as it is very weak compared to junctional myosin.

> *• Given the authors' observation of differences in the relative localization of KST and α Spec (Figure 4), proper quantification of KST, α Spec and myosin levels along the apical-basal cell axis would be important. This would also ease data interpretation.*

Response: We have now added a higher resolution image and also a line scan of Kst, α-Spec and Myo in a new supplemental figure (Fig 6 supplement 1)

> *• KD of α Spec seems to induce myosin activity more, causes a bigger reduction of wing thickness, a stronger induction of Jub, and a similar effect on wing size. What lead the authors to focus on KST rather than α Spec regarding the detailed analysis of myosin competition?*

Response: Our observations identify a competition between Kst and myosin, but we have no indication that α-Spec competes with myosin. (It's conceivable that β-Spec might also compete with myosin in some contexts, but wing discs would not be a good place to examine this because the localization profiles of β-Spec and Myosin are so different).

> *• A big criticism regarding the figures is the bad color choice which makes it difficult to decipher the fluorescent signals. Likewise, the labels are difficult to read with the present coloring. They should really be changed.*

Response: We have now changed the single color images to gray scale (for multi-color images we retain RGB coloring).

> *A minor point:*
>
> *• To make the manuscript more accessible for researchers outside the Drosophila field, I'd suggest adding explanatory labels for Drosophila-specific terms such as hyperactive myosin for sqhEE, a scheme to show where UAS-dcr2 is active, explain the purpose of Rfp expression as a control for tissue specificity, etc.*

Response: We have added some explanations to the text to try to make this clearer.

> ## *Reviewer #2 (Recommendations For The Authors):*
>
> ***Major points:***
>
> *In lines 99-101, the authors mention that Deng et al., 2015 report that the depletion of spectrins leads to an increase in pMLC, with no associated changes in the colocalization of myosin and F-actin. It is more accurate to mention that Deng et al. suggest that the levels of a GFP-tagged rescue construct of MLC (Sqh) are unchanged in alpha-spectrin mutants, although this was not formally quantified. Moreover, there was not a formal assessment of colocalization between MLC and F-actin, but rather a suggestion that F-actin levels are unaffected by the alpha-spectrin mutation. Finally, Deng et al. mostly analyzed alpha-spectrin so it remains possible that the new results shown by the authors are compatible with the initial observations from Deng and colleagues.*

Response: As suggested, we revised the text to note that Deng et al., 2015 specifically examined Sqh:GFP. While we agree that our focus is more on Kst and Deng et al focused on α-

Spec, we also examined α-Spec, and as described our results examining Myosin and Jub differ from what was reported by Deng et al 2015.

> *As mentioned above, it is still possible that spectrins and Ajuba are working in parallel and Ajuba is not necessarily downstream of spectrins. The strong phenotype of Ajuba RNAi flies in adult wings could mask the effect of spectrins. Are the results similar in other settings, such as in the absence of Dicer2? Also, can Ajuba RNAi phenotypes be modified by overexpression of spectrins? This would provide further evidence of a link to Ajuba function.*

Response: While formally it is true that the genetic requirement for Jub could reflect a role in parallel to, rather than downstream of, spectrins, our conclusion that spectrins act through Jub is based not only on the genetic requirement for Jub, but also on the influence of spectrins on junctional tension and Jub localization, which indicate that spectrins influence Jub activity in a manner consistent with their affecting the Hippo pathway through Jub.

We would not expect over-expression of spectrins in a jub RNAi background to further reduce Hippo signaling, and as the jub RNAi phenotype is much stronger than the Kst over-expression phenotype even if there were an effect it would likely be difficult to detect.

> *Regarding the potential independent functions of spectrins, it would be interesting to determine if alpha- and beta-heavy-spectrin can still interact at the level of the AJ despite the fact that their distributions appear to be partly non-overlapping. Would it be possible to assess this using PLA? If an interaction is not detected via PLA, it would be more convincing that spectrins are functioning independently.*

Response: We have now performed this experiment, and no significant signal was detected by PLA. As a control, we used identical antibodies (GFP and α-Spec) to conduct PLA on α-Spec and β-Spec, and we did detect signal by PLA. These results (included in a revised Figure 4) further support the conclusion that α-Spec and βH-Spec are not physically associated in wing discs.

> *Related to this point, if the spectrins work independently, it is reasonable to assume that they could display additive effects. Is this the case? If alpha- and beta-heavy-spectrin are simultaneously depleted are the phenotypes more severe than either depletion alone?*

Response: We disagree here. Since both alpha- and beta-heavy-spectrin act through tension and Jub, and there is likely a limit as to how much Yki activity can be increased by this pathway. For example, the increases in wing size induced by spectrin RNAi are similar to the increases in wing size observed with constitutive recruitment of Jub through alpha-catenin mutation (Alegot et al 2019), which may thus represent the maximum increase that can be induced through this pathway (as there are multiple, independent factors that regulate Hippo signaling).

> *Authors should modulate membrane tension and assess if this affects the localization of alpha- and beta-heavy-spectrin and, specifically, their colocalization, as their interaction could be regulated.*

Response: As reported, we do see effects of tension on βH-Spec localization. We would not expect significant effects of membrane tension on α-Spec localization, but we consider analysis of this outside the scope of this manuscript.

> *In lines 185-187, the authors mention that beta-spectrin depletion does not affect beta-heavy-spectrin localization. Interestingly, Figure 4E appears to show that the levels of Kst-YFP appear to be lower in the beta-spectrin-depleted tissue. The localization of beta-heavy-spectrin is not necessarily affected but the overall levels could be.*

Response: Indeed the levels appear slightly lower, but elucidating the reason for this will require further experiments that are beyond the scope of this manuscript (we suspect it is

because cytoskeletal tension increases in β-Spec-depleted tissue as it does in α-Spec depleted tissue, which based on our observations should decrease levels of Kst at near junctions). The key point of these experiments was to show that α-Spec localization does not require βH-Spec, but does require β-Spec, which supports our conclusion that in wing discs α-Spec forms a complex with β-Spec but not with βH-Spec.

> *In lines 200-203, the authors state that beta-heavy-spectrin and myosin colocalize extensively at the apical region. However, this colocalization is not as clear as stated. Do the authors have alternative data that suggests that the two proteins are indeed colocalizing? Would it be possible to perform PLA to detect a potential colocalization?*

Response: Unfortunately we do not have antibodies against both proteins that work well enough for PLA. However, we quantified the co-localization by analysis of Pearson's correlation coefficient, as reported in the manuscript. We also added an additional higher magnification image, and a line scan, in a supplemental figure (Fig. 6 supplement 1).

> *Authors should try to assess and quantify colocalization with F-actin for both beta-heavy-spectrin and myosin in wild-type conditions and when the levels (and/or activity) for each of them are modulated.*

Response: We have added quantification of the co-localization of βH-Spec with F-actin and of myosin with F-actin to the revised manuscript.

> *Minor points:*
>
> *In lines 122-124, the authors should clarify the relevance of the observation that alpha-spectrin knockdown affects the thickness of the wing disc epithelium.*

Response: We have added some text to try to elaborate on this.

> *In the intro, it is perhaps necessary to mention that there are conflicting reports regarding the role of spectrins in the regulation of cell proliferation, at least in the follicular epithelium. For instance, Ng et al., 2016 argued that spectrins do not regulate cell proliferation in FECs.*

Response: Rather than wading into a detailed discussion of issues that are peripheral to this study, we modified the text in the Introduction to avoid implying that spectrins control cell proliferation in the ovary.

> *In Figures 1, 2, 3, and 4 (and respective supplements), it is encouraged that, wherever appropriate, the authors mark the different compartments or the relevant boundary using dashed lines, to more clearly indicate the regions to compare.*

Response: We have now done this.

> *In Figure 2, supplement 1 panels C and D should have an indication of the genotype for clarity.*

Response: We have now added this.

> *In lines 362-367, the authors suggest that other actin-binding proteins are likely to influence the role of beta-heavy-spectrin. Have the authors tested the role of spectrin interactors such as Ankyrin and Adducin?*

Response: No, we have not examined this.